



Data-Driven Modeling and Neural Network Solver

Zhiliang Xu

z xu2@nd.edu

Department of Applied and Computational Mathematics and Statistics
University of Notre Dame, Notre Dame, IN 46556

ALLDATA 2022. April 25-28, 2022

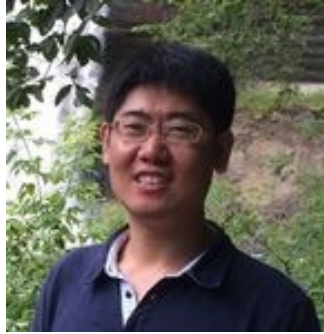
π





- Ph.D., State University of New York at Stony Brook, 2002
- M.S., Beijing University of Aerospace and Astronautics, China, 1997
- Dr. Xu's research interests include 1) using computational and mathematical modeling to study problems arising from physics and biology; 2) developing high-order accurate and efficient numerical schemes for solving PDEs arising in modeling classical fluid dynamics and complex fluids problems.

Acknowledgement



Shixin Xu¹



Chun Liu²



Mark Alber³



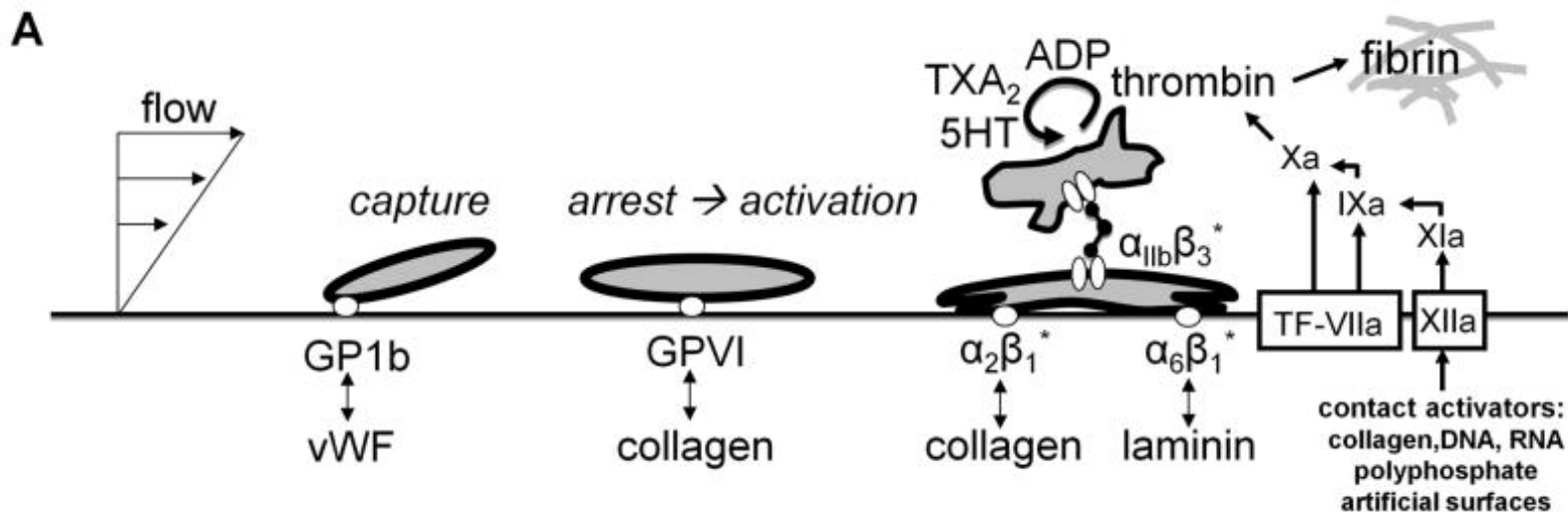
John Weisel⁴

1. Department of Mathematics, DKU
2. Department of Applied Mathematics, IIT
3. Department of Mathematics, UC Riverside
4. Department of Cell and Development Biology, U. Penn



Outline

- › Background of blood clotting
- › A continuum mechanistic model for studying stability of blood clot
- › Background of vesicles
- › A continuum microscale model for vesicle motion and deformation
- › Concluding remarks



Autocatalytic deposition of platelets on an injured vascular wall and generation of coagulation proteases

A. Adhesion of platelet to vWF mediates capture under flow conditions, followed by platelet activation via GPVI.

Ref. Annu Rev Biomed Eng. 2013;15:283-303.

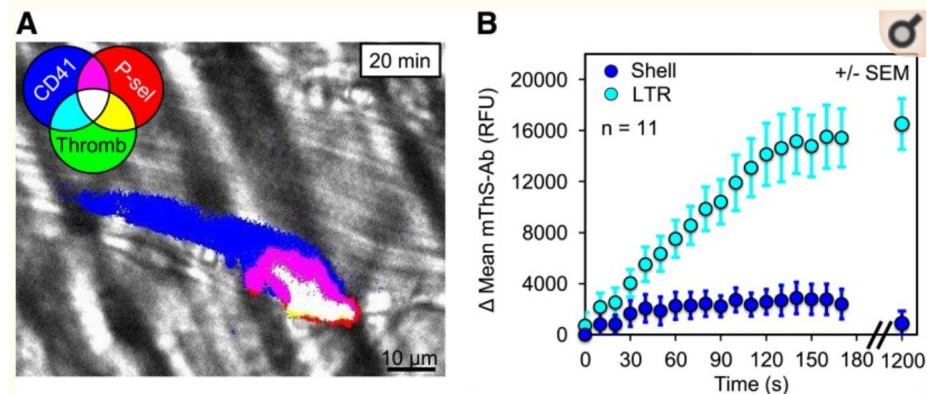
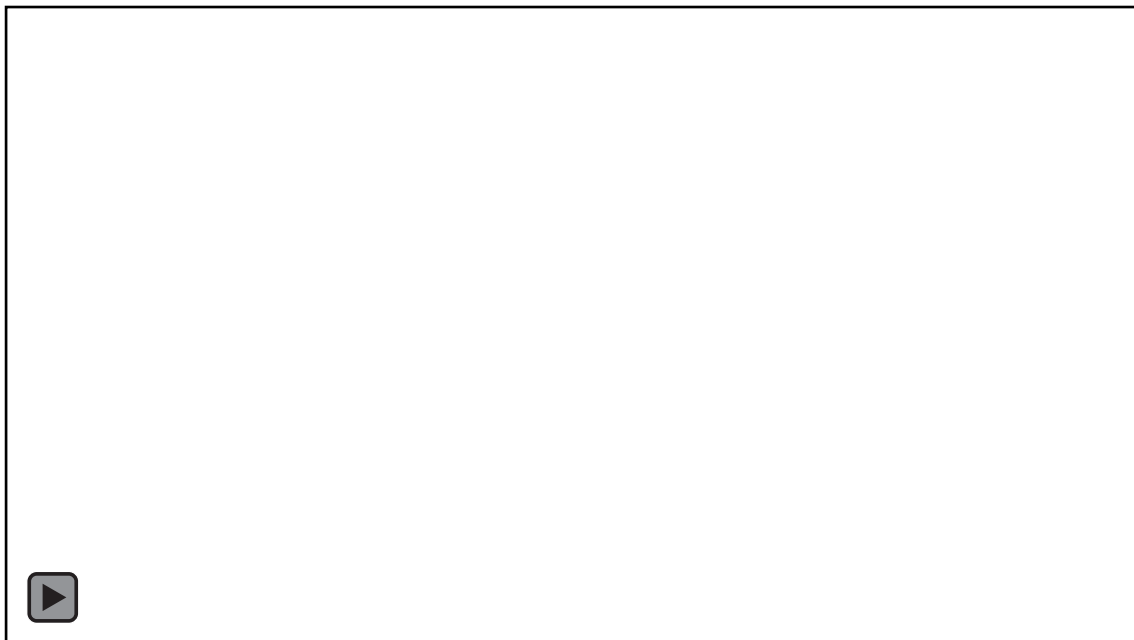
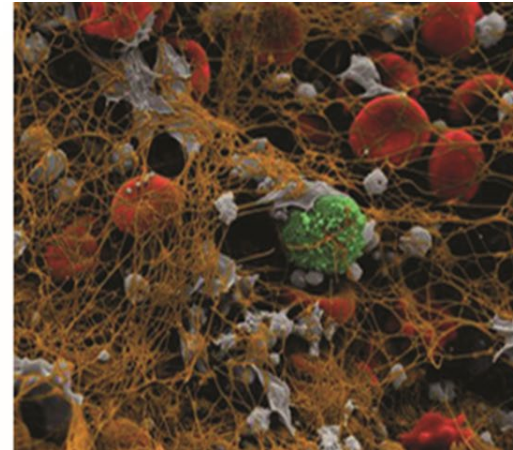
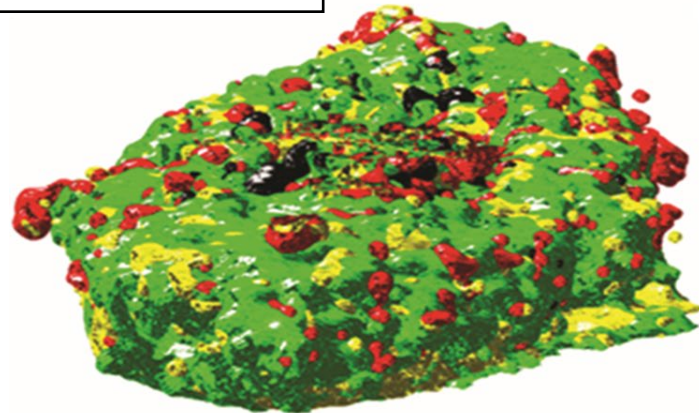


Figure 5

Thrombin activity within the LTR. (A) A representative image of thrombin activity (mThS-Ab; green, binary mode) within a thrombus 20 minutes after injury also showing platelet deposition (blue) and core formation (red). Overlay of 3 channels is white. (B) The change in the mean mThS-Ab fluorescence was monitored within the LTRs (cyan) and shell (blue) during the initial 3 minutes after injury and again at 20 minutes (\pm SEM).

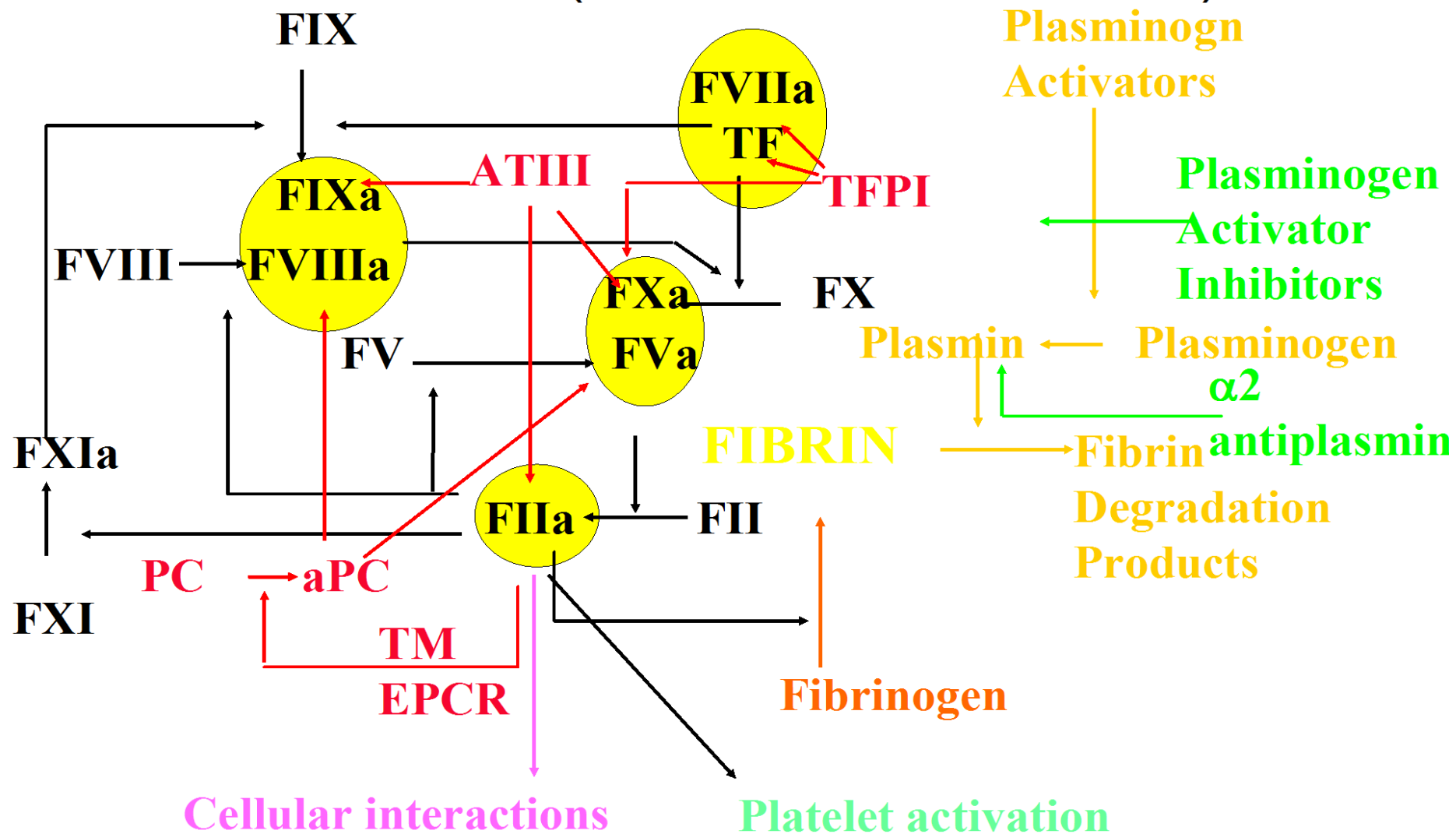
[Open in a separate window](#)

Top: 3D Reconstruction of a Clot from z-stacks by Confocal-microscopy.



Left) 3D image of a late stage thrombus: regions composed mostly of platelets are red, mostly of fibrin-green, mostly of platelets and fibrin are yellow; and other material and cells are black;

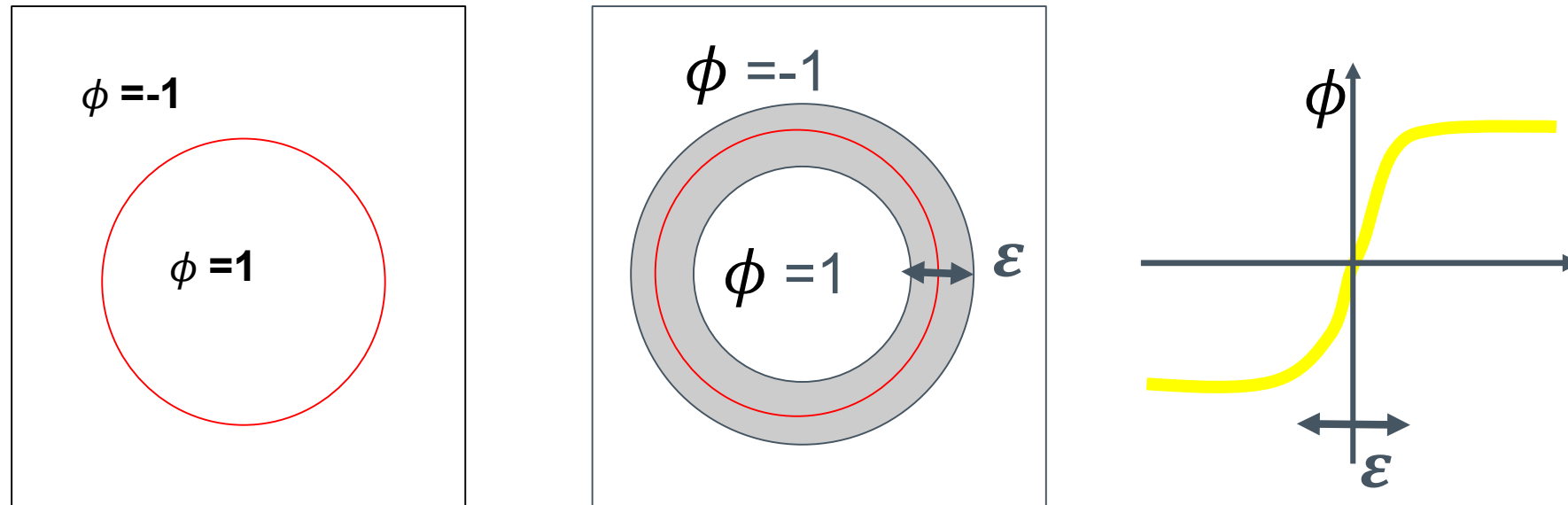
Right) Colorized scanning electron micrograph taken from the patient who had a heart attack. Fibrin fibers are brown, red blood cells are red, leukocytes are green, platelets are depicted in gray.



Network of Coagulation Reactions. Xu *et al.* A Multiscale Model of Venous Thrombus Formation with Surface-Mediated Control of Blood Coagulation Cascade, *Biophysical Journal*, 19;98(9):1723-32, 2010.

Diffuse Interface/Phase-Field

- › Lord Rayleigh (1892) and van der Waals (1893).
- › A **phase field function** (order parameter) ϕ is used to label material on two sides of the interface, with nearly constant values except in a thin layer (the diffuse interface layer).



(left) Sharp Interface. (Middle) Diffuse interface. (Right) ϕ value in diffuse interface model.

- The diffuse-interface model and the sharp interface model are also related.

Let $f_0(\phi) = \frac{\lambda}{4\epsilon^2} (\phi^2 - 1)^2$. In 1D, consider to require the diffuse mixing energy be equal to the classical surface energy (surface tension): $\sigma = \lambda \int_{-\infty}^{\infty} \left\{ \frac{1}{2} \left(\frac{d\phi}{dx} \right)^2 + \right.$



Energetic Variational Approach

π

The starting point is the **energy dissipation law**:

$$\frac{d}{dt} E^{total} = -\Delta$$

Where E^{total} includes both kinetic and free internal energy [1, 2].

Δ is the dissipation functional.

- When $\Delta = 0$, the total energy is conserved.
- This law can be derived from the first and second law of thermodynamics.
 - The 1st law: $\frac{d(K+U)}{dt} = \frac{dW}{dt} + \frac{dQ}{dt}$. Here K is the kinetic energy, U is internal energy, W is the work and Q is the heat.
 - The 2nd law in isothermal case: $T \frac{dS}{dt} = \frac{dQ}{dt} + \Delta$. T is temperature, S entropy. $\Delta \geq 0$ is the entropy production.

› [1]. L. Onsager. 1931. Phys. Rev.

› [2]. J. Forster, Mathematical Modeling of Complex Fluids, 2013.

Least Action Principle

π

Let $F := U - TS$ be the Helmholtz free energy.

Let $L := K - F$ be the Lagrangian function of a conservative system. The *action functional* for this system is defined by

$$A(\mathbf{x}(t)) := \int_0^{t^*} L(\mathbf{x}(t), \mathbf{x}_t(t)) dt .$$

Least action principle (LAP): the equation of motion for a Hamiltonian (conservative) system can be obtained by taking the variation of the action functional with respect to the flow maps $\mathbf{x}(t)$.

› Or $\delta(E^{total}) = \mathbf{force}_{consrv} \cdot \delta(\mathbf{x})$

Maximum Dissipation and Force Balance

π

The maximum dissipation principle gives rise to the dissipative force of the system.

The maximum dissipation principle: the dissipative force can be obtained by taking the variation of the dissipation functional with respect to the rate such as the velocity.

$$\longrightarrow \frac{\delta \left(\frac{1}{2} \Delta \right)}{\delta(\dot{\mathbf{x}}_t)} = \mathbf{force}_{dissipative}$$

Force Balance: $\mathbf{force}_{dissipative} = \mathbf{force}_{consrv}$

The Spring System

By Newton's law: $mx_{tt} + \gamma x_t + kx = 0$

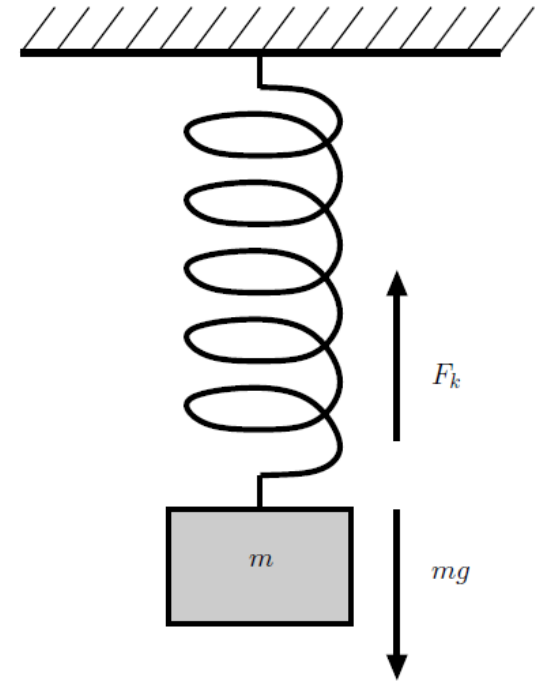
$$K = \frac{1}{2}mx_t^2,$$

$$F = \frac{1}{2}kx^2.$$

$$A(x(t)) := \int_0^{t^*} (K - F)dt.$$

Apply LAP:

$$force_{consrv} = -mx_{tt} - kx.$$



The dissipation due to friction:

$$\Delta = \gamma x_t^2.$$

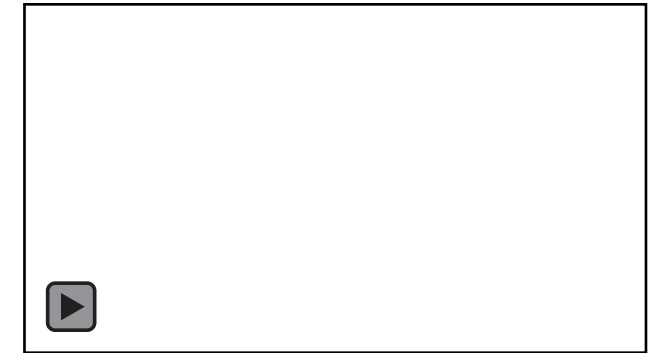
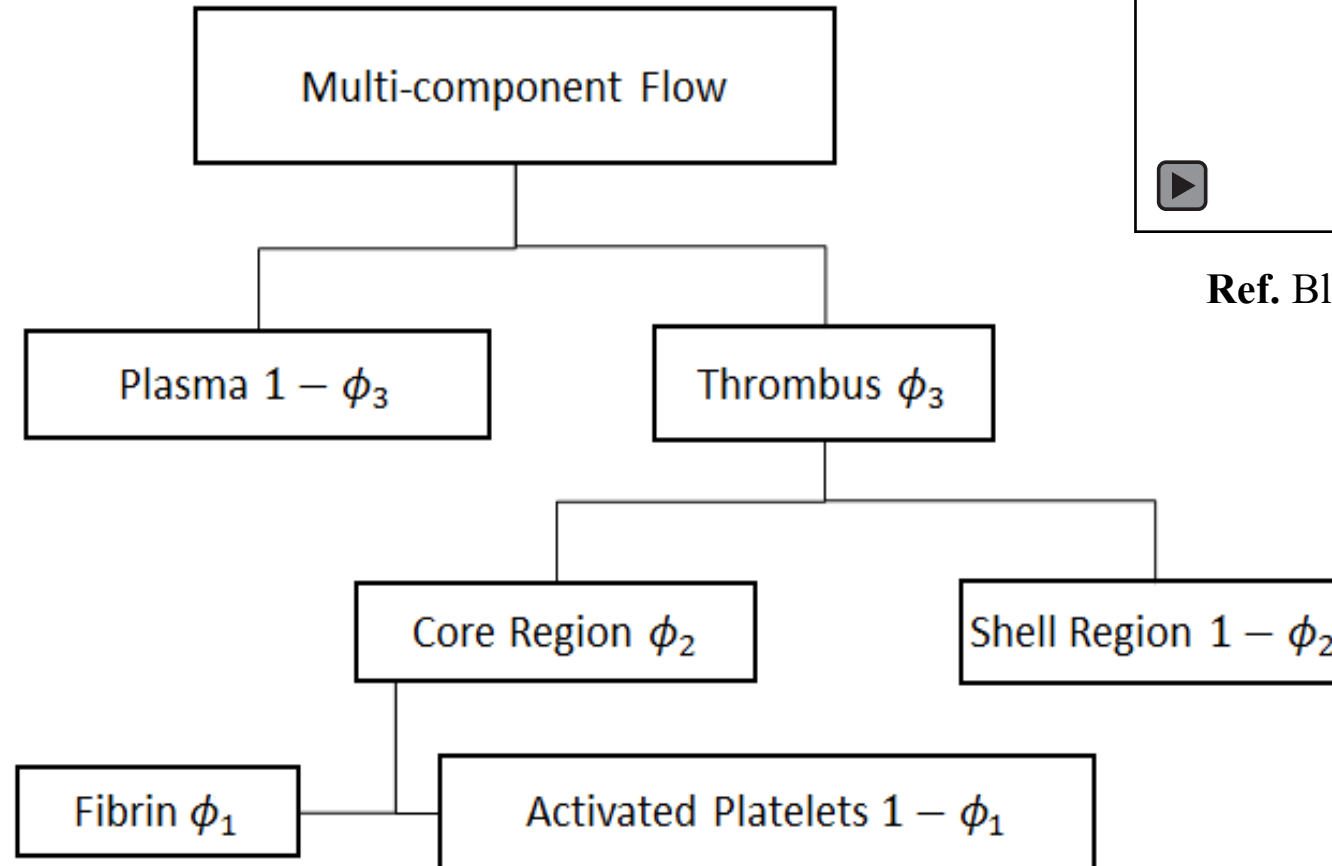
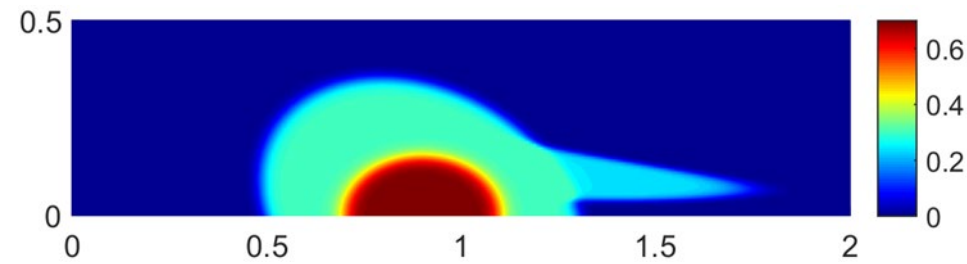
The maximum dissipation principle:

$$force_{dissipative} = \gamma x_t.$$

Force Balance:

$$-mx_{tt} - kx = \gamma x_t.$$

Binary tree structure to construct multi-component clot system



Ref. Blood. 124(11) 2014.

Derivation of the Multi-component System

π Let ϕ_1 ($\phi_1 \in [0,1]$) be the volume fraction of fibrin network in the core of the blood clot, a viscoelastic mixture; ϕ_2 ($\phi_2 \in [0,1]$) be volume fraction of the core of the blood clot; and ϕ_3 ($\phi_3 \in [0,1]$) be volume fraction of the blood clot of the system. The blood clot is viscoelastic, and is modeled by the Kelvin-Voigt model.

The total energy functional E_{tot} is defined as follows:

$$E_{tot} = E_{kin} + E_{coh1} + E_{coh2} + E_{coh3} + E_{ela}.$$

Here

$$E_{kin} = \int_{\Sigma} \frac{1}{2} \rho |\mathbf{u}|^2 dx;$$

$$E_{ela} = \int_{\Sigma} \frac{\lambda_e}{2} |\mathbf{F}|^2 dx \text{ with } \lambda_e = \phi_3 \left(\phi_2 \left(\phi_1 \lambda_{e,n} + (1 - \phi_1) \lambda_{e,p} \right) + (1 - \phi_2) \lambda_{e,s} \right)$$

$\mathbf{F} = \frac{\partial \mathbf{x}}{\partial \mathbf{X}}$, is the deformation gradient tensor.

$\lambda_{e,n}$, $\lambda_{e,p}$ and $\lambda_{e,s}$ are elastic energy density of fibrin, activated platelets and less-activated platelets, respectively.

Interaction between platelets and fibrin:

$$E_{coh1} = \int_{\Sigma} \lambda_1 \phi_2 \phi_3 (G_1(\phi_1) + \frac{\gamma_1^2}{2} |\nabla \phi_1|^2) dx;$$

Interaction between core and shell regions of the clot:

$$E_{coh2} = \int_{\Sigma} \lambda_2 \phi_3 (G_2(\phi_2) + \frac{\gamma_2^2}{2} |\nabla \phi_2|^2) dx;$$

Interaction between the clot and plasma:

$$E_{coh3} = \int_{\Sigma} \lambda_3 (G_3(\phi_3) + \frac{\gamma_3^2}{2} |\nabla \phi_3|^2) dx .$$

Here $G_i = \frac{1}{4} \phi_i^2 (1 - \phi_i)^2$.

F satisfies:

$$F_t + \mathbf{u} \cdot \nabla F = \nabla \mathbf{u} \cdot F.$$

In 2D, assume $\nabla \cdot F(t = 0) = 0$. There exists a matrix Ψ which satisfies:

$$\begin{cases} \partial_t \Psi + \mathbf{u} \cdot \nabla \Psi = 0, \\ F = \nabla \times \Psi. \end{cases}$$

To this end, the elastic energy is represented as:

$$E_{ela} = \int_{\Sigma} \frac{\lambda_e}{2} |\nabla \Psi|^2 dx.$$

The dissipation of the system is assumed to be given by:

$$\Delta = \int \left[\frac{\eta}{2} |D|^2 + \frac{\eta\phi_3}{\kappa} |u|^2 + \tau_1 |\nabla\mu_1|^2 + \tau_2 |\nabla\mu_2|^2 + \tau_3 |\nabla\mu_3|^2 \right] d\mathbf{x}.$$

$D = \nabla\mathbf{u} + (\nabla\mathbf{u})^T$ is $(2\times)$ the strain rate tensor.

τ_i is the phenomenological mobility coefficient.

$\mu_i = \frac{\delta E_{tot}}{\delta\phi_i}$ is the chemical potential.

κ is the permeability of the clot and is approximated by $\frac{1}{\kappa} = \frac{1-\phi_2}{\kappa_S} + \frac{\phi_2}{\kappa_C}$.

κ_S : shell region; κ_C : core region.

$$\begin{aligned}\phi_1 + \nabla \cdot (\mathbf{u} \nabla \phi_1) &= \nabla \cdot (\tau_1 \nabla \mu_1), \\ \phi_2 + \nabla \cdot (\mathbf{u} \nabla \phi_2) &= \nabla \cdot (\tau_2 \nabla \mu_2), \\ \phi_3 + \nabla \cdot (\mathbf{u} \nabla \phi_3) &= \nabla \cdot (\tau_3 \nabla \mu_3),\end{aligned}$$

$$\mu_1 = \frac{\partial_{\phi_1} \lambda_e}{2} |\nabla \Psi|^2 + \lambda_1 \phi_3 \phi_2 G'_1(\phi) - \lambda_1 \gamma_1^2 \nabla \cdot (\phi_2 \phi_3 \nabla \phi_1),$$

$$\mu_2 = \frac{\partial_{\phi_2} \lambda_e}{2} |\nabla \Psi|^2 + \lambda_2 \phi_3 G'_2(\phi_2)$$

$$- \lambda_2 \gamma_2^2 \nabla \cdot (\phi_3 \nabla \phi_2) + \phi_3 (\lambda_1 G_1(\phi_1) + \lambda_1 \frac{\gamma_1^2}{2} |\nabla \phi_1|^2),$$

$$\mu_3 = \frac{\partial_{\phi_3} \lambda_e}{2} |\nabla \Psi|^2 + \lambda_3 G'_3(\phi_3) - \lambda_3 \gamma_3^2 \Delta \phi_3$$

$$+ 2(\lambda_2 G_2(\phi_2) + \lambda_2 \frac{\gamma_2^2}{2} |\nabla \phi_2|^2) + \phi_2 (\lambda_1 G_1(\phi_1) + \lambda_1 \frac{\gamma_1^2}{2} |\nabla \phi_1|^2).$$

Where ∂_i denotes ∂_{ϕ_i} .

$$\rho(\partial_t \mathbf{u} + (\mathbf{u} \cdot \nabla) \mathbf{u}) + \nabla P = \mathbf{F}_{vis} + \mathbf{F}_{coh} + \mathbf{F}_{ela}$$
$$\nabla \cdot \mathbf{u} = 0$$

where

$$\mathbf{F}_{vis} = \nabla \cdot (\eta D) - \frac{\eta \phi_3}{\kappa} \mathbf{u} ,$$

$$\mathbf{F}_{coh} = -\lambda_3 \gamma_3^2 \nabla \cdot (\nabla \phi_3 \otimes \nabla \phi_3) - \lambda_2 \gamma_2^2 \nabla \cdot (\phi_3 \nabla \phi_2 \otimes \nabla \phi_2)$$
$$- \lambda_1 \gamma_1^2 \nabla \cdot (\phi_2 \phi_3 \nabla \phi_1 \otimes \nabla \phi_1) ,$$

$$\mathbf{F}_{ela} = -\nabla \cdot (\lambda_e \nabla \Psi^T \nabla \Psi)$$

See also Supplementary Material in: *Xu et al. 2017 J.R. Soc. Interface.*

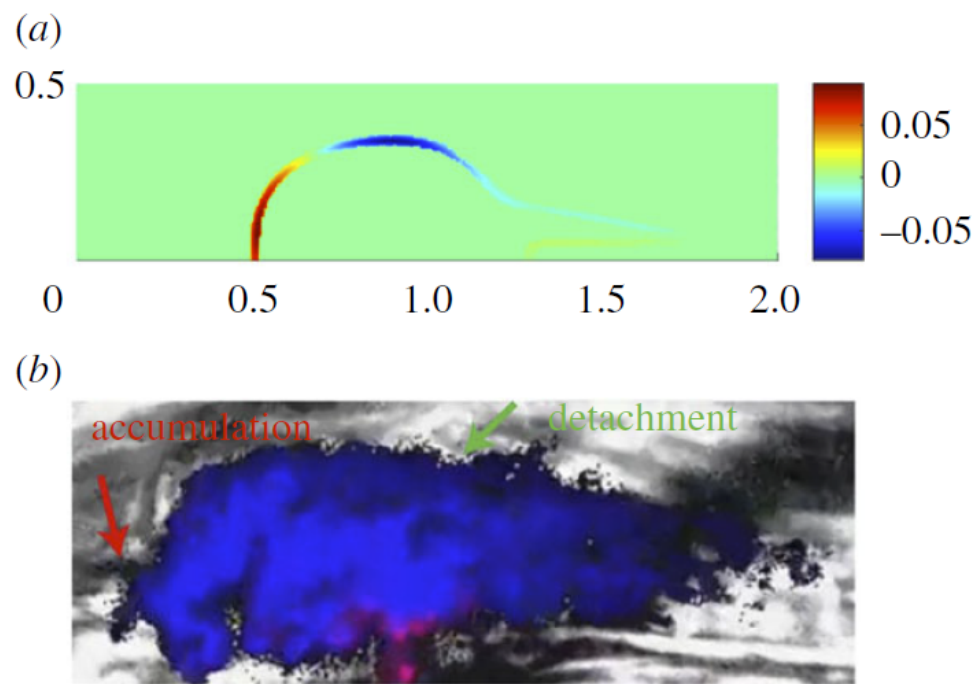


Figure 4. Accumulation and detachment of free-flowing platelets over the surface of the blood clot. (a) Simulated distribution of the magnitude of the rate function S_g (s^{-1}) on the surface of the blood clot with shell permeability $K_s = 10^{-12} \text{ m}^2$ at shear rate $\dot{\gamma} = 1000 \text{ s}^{-1}$. Platelet accumulation on the upstream surface of the clot is shown by the red zone. Platelet detachment zone on the clot surface is shown in blue. The unit of length is $L = 100 \text{ }\mu\text{m}$ (figure 3c). (b) A snapshot of the experimental movie showing the arterial clot formed *in vivo* (movie is provided as a supplementary information to [10]). Small dots indicate single platelets. Arrows show the locations of platelet accumulation on the upstream surface of the clot and of platelet detachment from the top portion of the clot surface. The region with platelet aggregates is indicated in blue colour and the domain with fibrin network in the core of the clot is indicated in red colour. (Online version in colour.)

Modeling platelets accumulation and detachment from clot surface

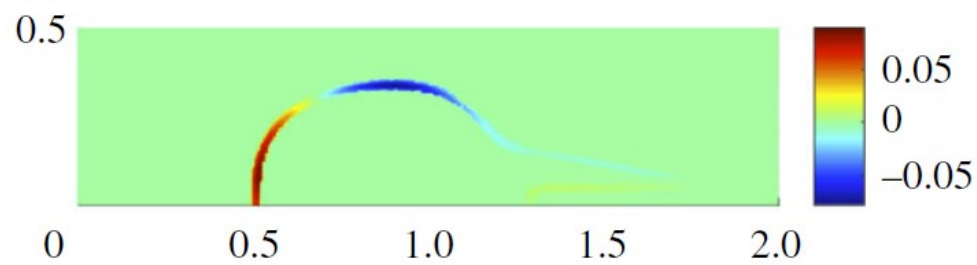
$$S_g(\mathbf{x}, t) = (\kappa_n \tau_n - \kappa_v \tau_v)$$

where \mathbf{x} is restricted to the surface of the blood clot; κ_n is the coefficient of platelet accumulation and κ_v is the coefficient of platelet detachment.

$\tau_n = \mathbf{n} \cdot (P\mathbf{I} - \eta(\nabla\mathbf{u} + (\nabla\mathbf{u})^T)) \cdot \mathbf{n}$ is the normal component of the flow stress on the blood clot surface;

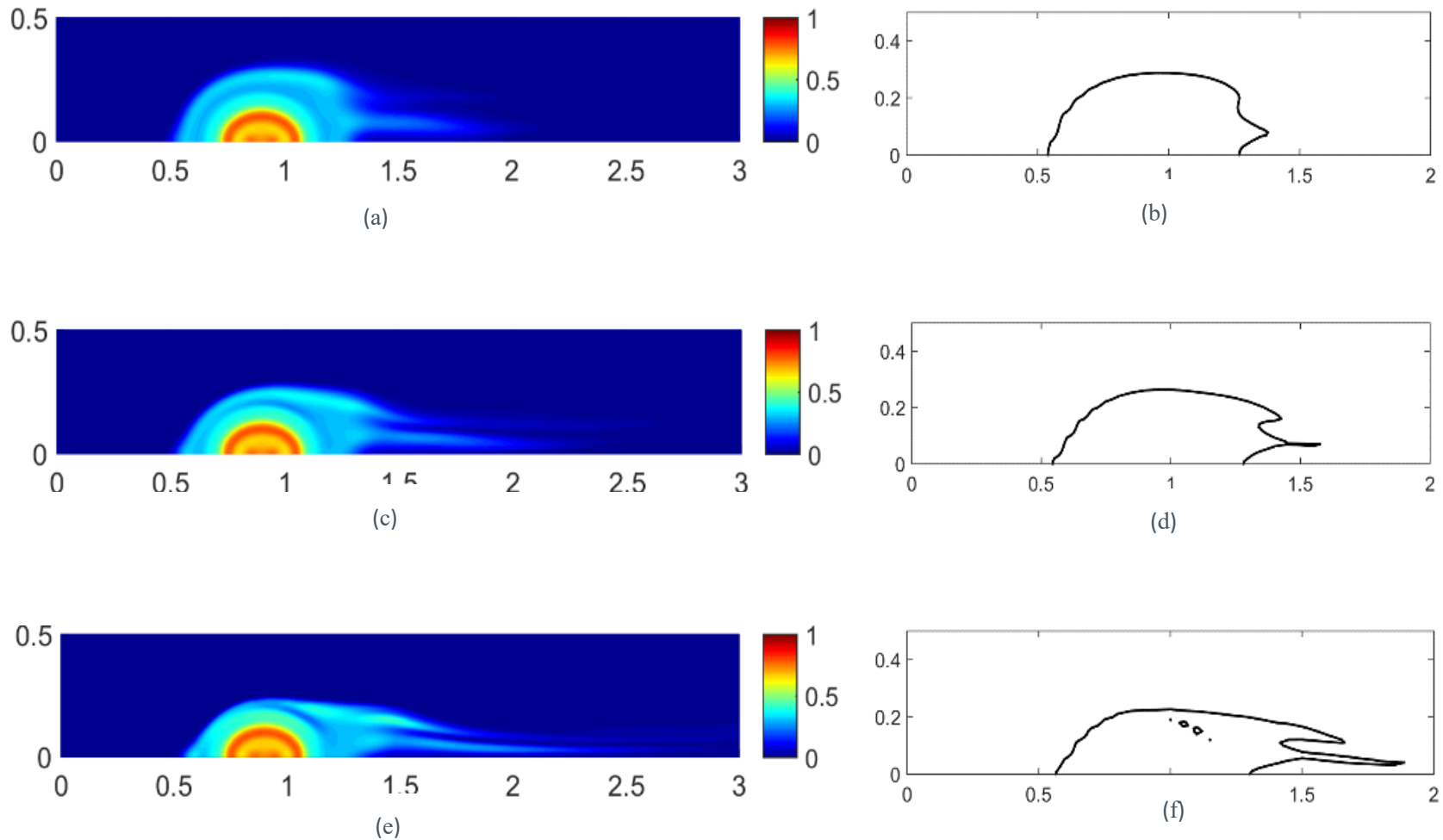
$\tau_v = \mathbf{v} \cdot (\eta(\nabla\mathbf{u} + (\nabla\mathbf{u})^T)) \cdot \mathbf{n}$ is the tangential component of the flow stress on the blood clot surface.

\mathbf{n} and \mathbf{v} are the normal and tangential vectors to the blood clot surface.

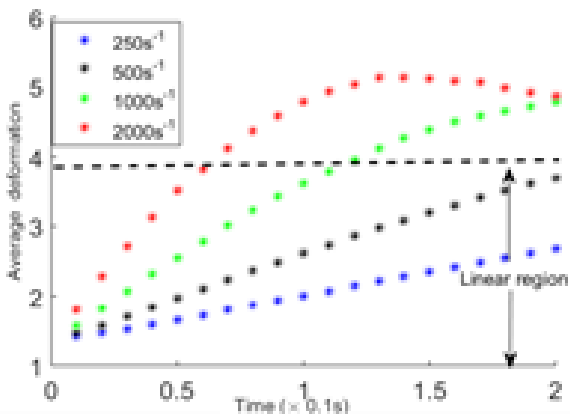


Effects of Flow Shear on Clot Deformation and Rupture

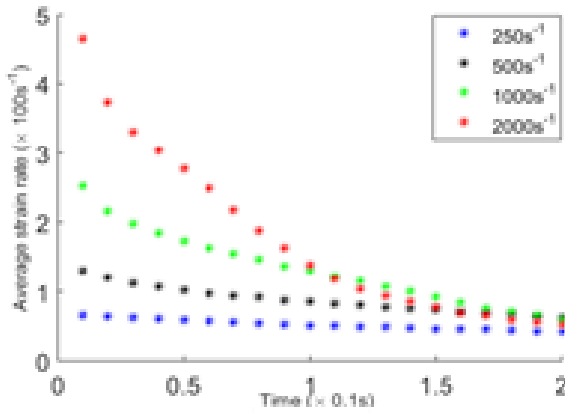
π



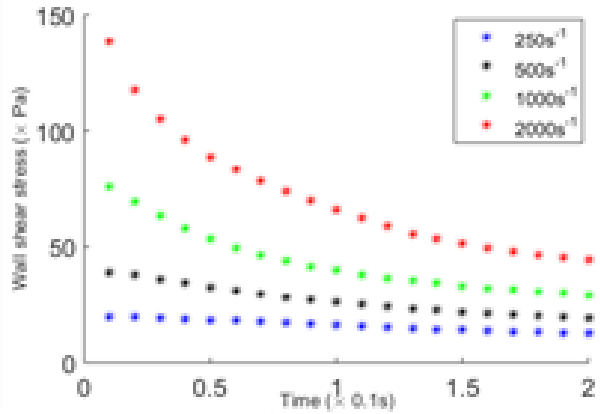
Simulation snapshots of blood clot deformation for different shear rate. Left column: volume fraction of blood clot. Right column: interface of the blood clot. First row: $\dot{\gamma} = 500 \text{ s}^{-1}$. Second row: $\dot{\gamma} = 1000 \text{ s}^{-1}$. Third row: $\dot{\gamma} = 2000 \text{ s}^{-1}$.



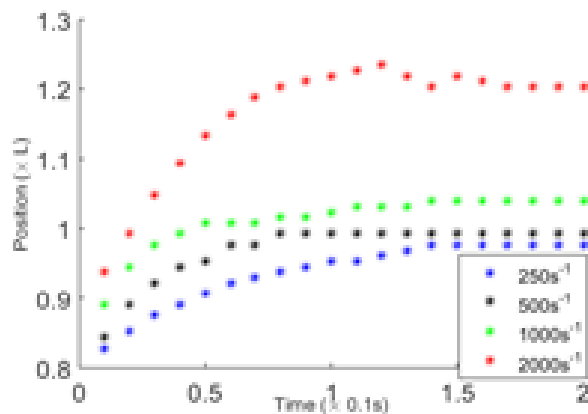
(a)



(b)



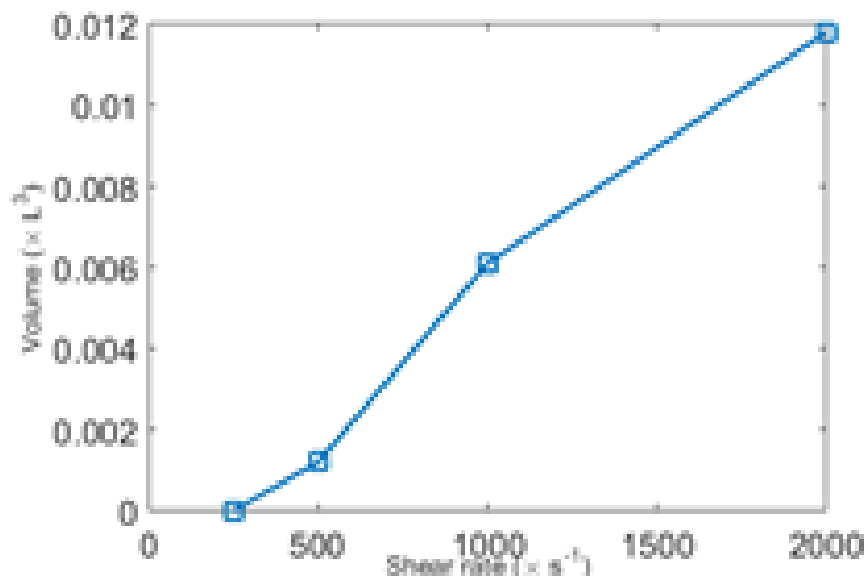
(c)



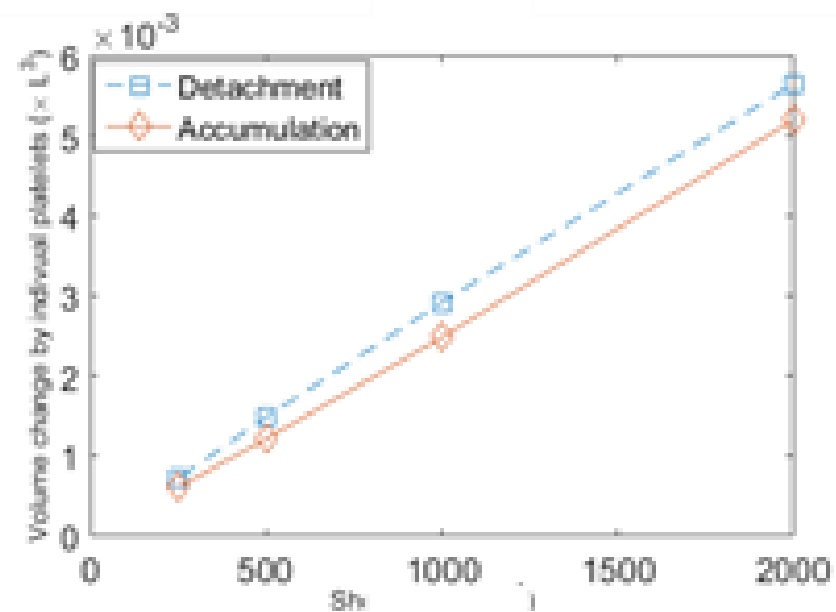
(d)

Effect of shear rate on blood clot deformation. (a) Average deformation tensor norm. (b) Average deformation rate norm. (c-d) Evolution of the maximum wall shear stress on the vessel wall and correspond position on the wall.

Average deformation gradient tensor: $\int_{\Omega_c} (\sum_{i,j=1,2} \mathbf{F}_{ij}^2)^{\frac{1}{2}} dx / Vol_c$, where $Vol_c = \int_{\Omega_c} \phi_3 dx$ is the volume of blood clot, Ω_c is the blood clot region and $\mathbf{F} = \frac{\partial \mathbf{x}}{\partial \mathbf{X}}$ is the deformation gradient tensor. Average deformation rate $\int_{\Omega_c} (\sum_{i,j=1,2} d_{ij}^2)^{\frac{1}{2}} dx / Vol_c$ with $d_{ij} = \frac{\partial_i u_j + \partial_j u_i}{2}$.



(e)



(f)

(e) Total volume of fragments passed through the observation cross section Γ .
(f) Rate of platelets accumulated on the surface of the blood clot and rate of platelets detached from the surface of the blood clot.

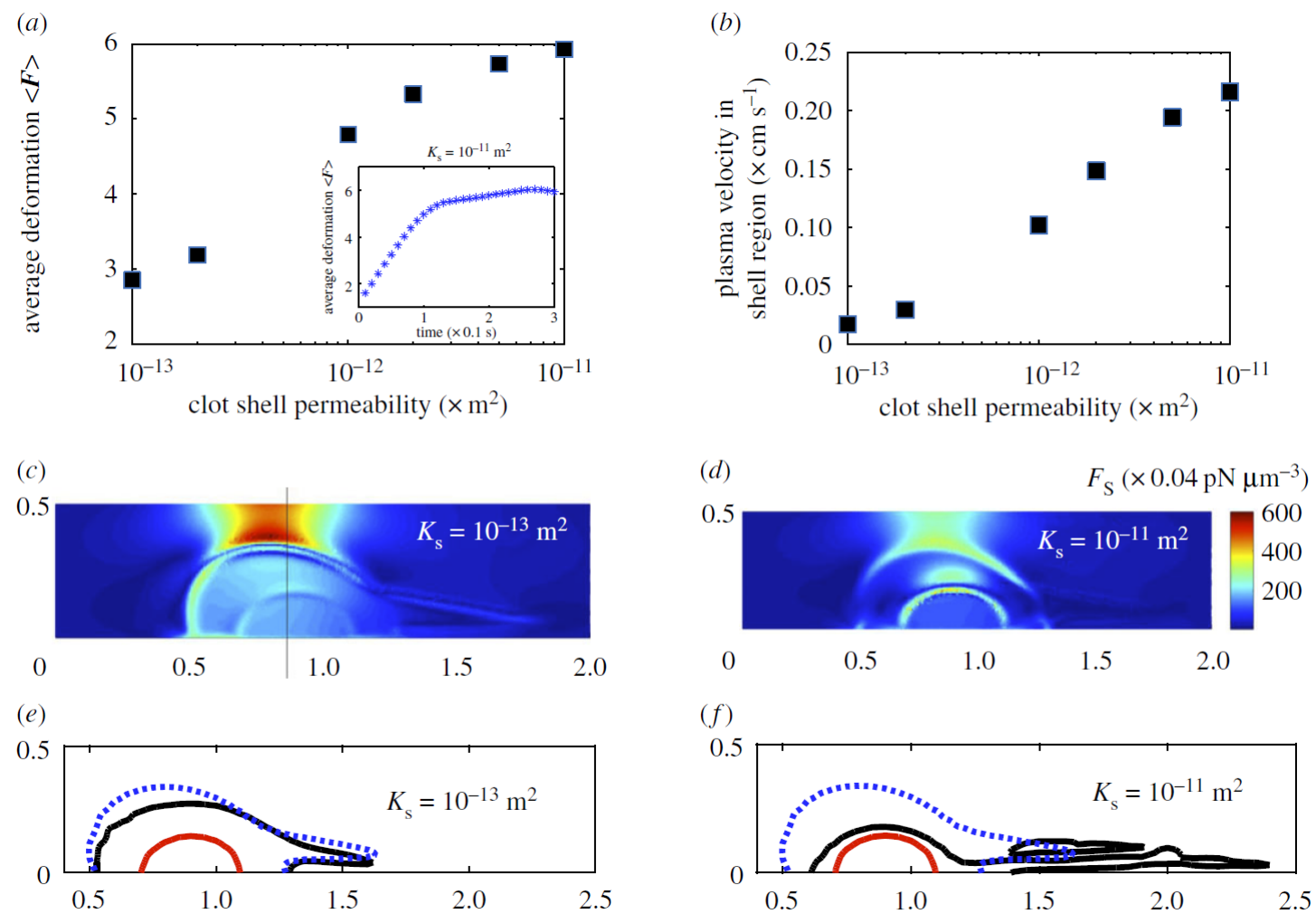


Figure 8. Effect of clot permeability on clot deformation, fragmentation and flow dynamics. (a) Volume averaged deformation tensor norm $\langle F \rangle$ as a function of clot shell permeability. The inset shows the evolution of the average deformation gradient tensor (DGT). (b) Relationship between mean plasma velocity in the clot shell region and shell permeability. (c,d) Spatial distribution of the shear force density induced by the flow over the clot with shell permeability $K_s = 10^{-13} m^2$ and $K_s = 10^{-11} m^2$, respectively, at time $t = 0.001 s$. (e,f) Flow-induced deformations of blood clots with shell permeability $K_s = 10^{-13} m^2$ and $K_s = 10^{-11} m^2$ at flow shear rate of $1000 s^{-1}$ at time $t = 0.3 s$. The black curve outlines the surface of the blood clot and its fragments. The red curve depicts the interface between the core and shell regions. The blue dot lines indicate initial interfaces. The unit of lengths are in terms of $L = 100 \mu m$ (figure 3). (Online version in colour.)

Table 2. Flow-induced clot volume dynamics for various clot permeability values under the blood flow with the shear rate $\dot{\gamma} = 1000 \text{ s}^{-1}$. Here $L = 100 \text{ }\mu\text{m}$.

permeability of the clot shell (10^{-13} m^2)	volume of accumulated platelets ($0.001 \times L^3$)	volume of detached platelets ($0.001 \times L^3$)	total fragment volume ($0.001 \times L^3$)	ruptured fragment volume ($0.001 \times L^3$)
100	3.2	3.1	18.1	8.5
50	3.1	3.0	15.1	5.3
20	3.1	3.4	12.4	0
10	3.4	3.8	11.2	0
2	3.9	4.5	8.4	0
1	4.1	5.3	7.4	0

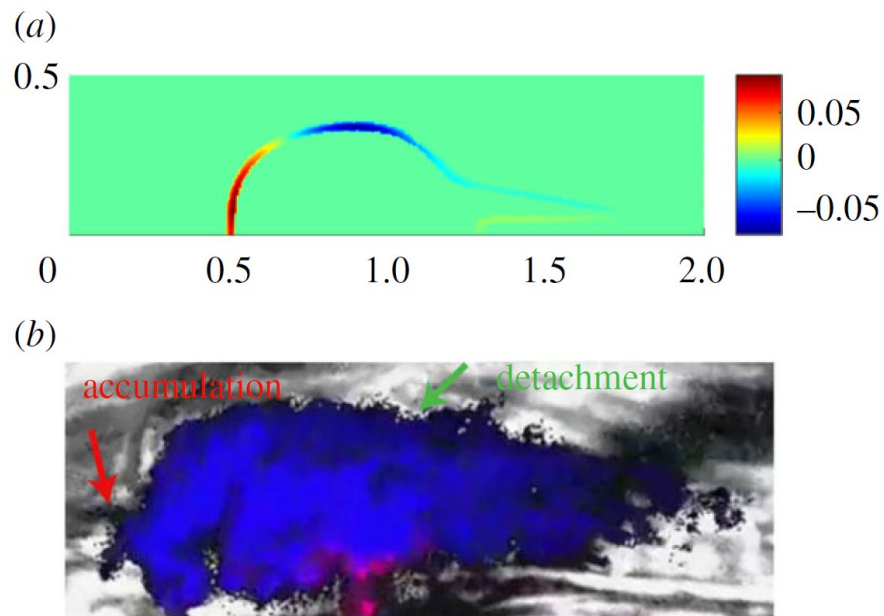
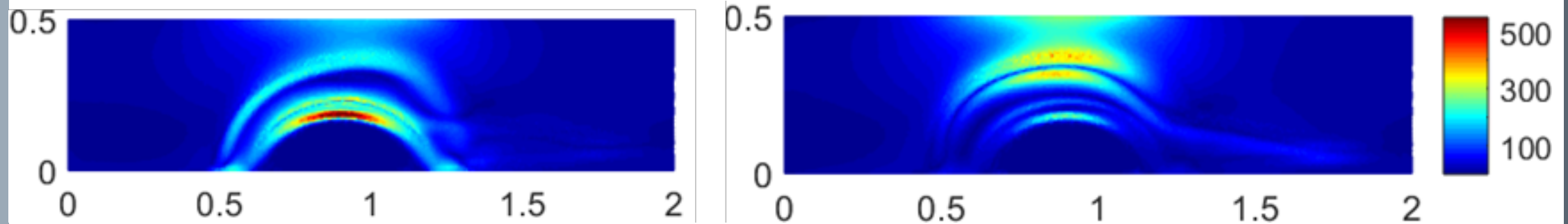


Figure 4. Accumulation and detachment of free-flowing platelets over the surface of the blood clot. (a) Simulated distribution of the magnitude of the rate function $S_g \text{ (s}^{-1}\text{)}$ on the surface of the blood clot with shell permeability $K_s = 10^{-12} \text{ m}^2$ at shear rate $\dot{\gamma} = 1000 \text{ s}^{-1}$. Platelet accumulation on the upstream surface of the clot is shown by the red zone. Platelet detachment zone on the clot surface is shown in blue. The unit of length is $L = 100 \text{ }\mu\text{m}$ (figure 3c). (b) A snapshot of the experimental movie showing the arterial clot formed *in vivo* (movie is provided as a supplementary information to [10]). Small dots indicate single platelets. Arrows show the locations of platelet accumulation on the upstream surface of the clot and of platelet detachment from the top portion of the clot surface. The region with platelet aggregates is indicated in blue colour and the domain with fibrin network in the core of the clot is indicated in red colour. (Online version in colour.)

Effects of Permeability and Porosity of Shell Region on Structural Stability of Clot



Magnitude of the shear force density of the flow $|\nabla \cdot \mathbf{D}|$ ($\times 0.04 pN/\mu m^3$) at time 0.01s. Left: $K_s = 10^{-11} m^2$. Right: $K_s = 10^{-12} m^2$.

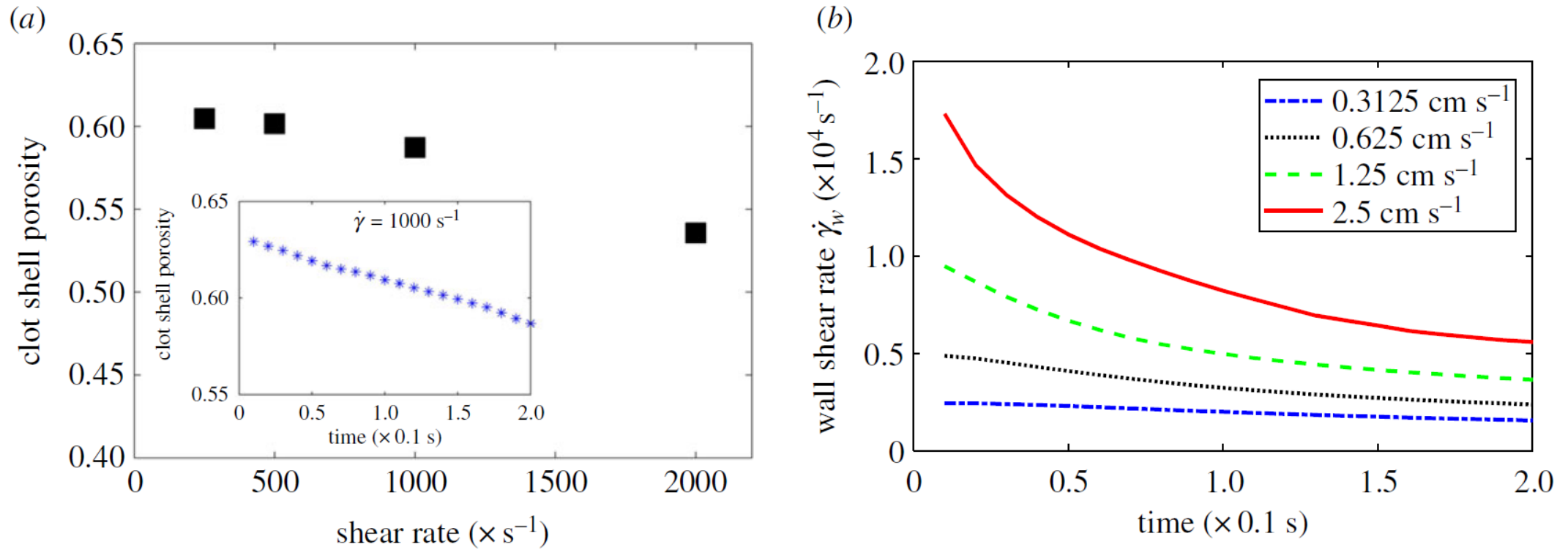
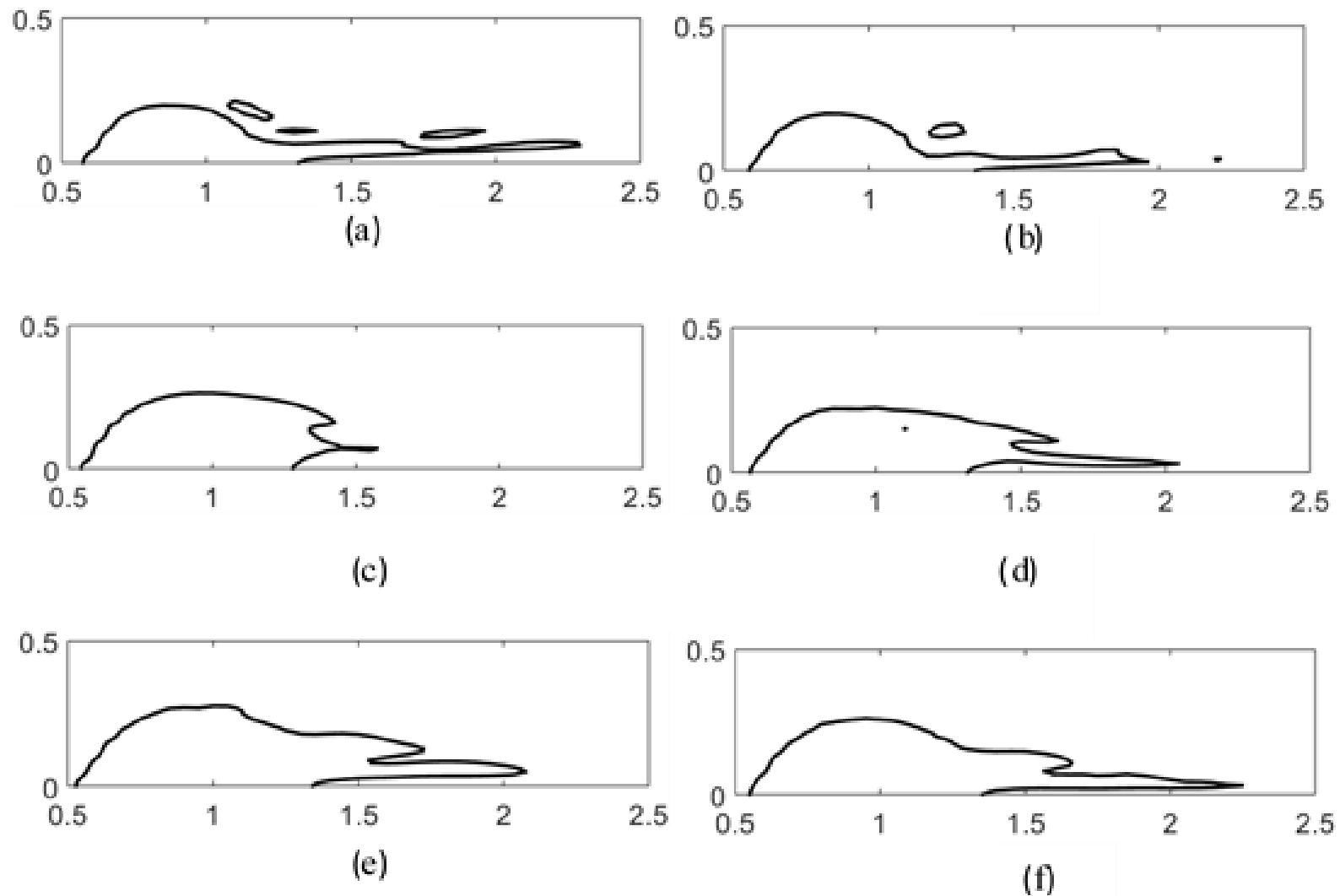
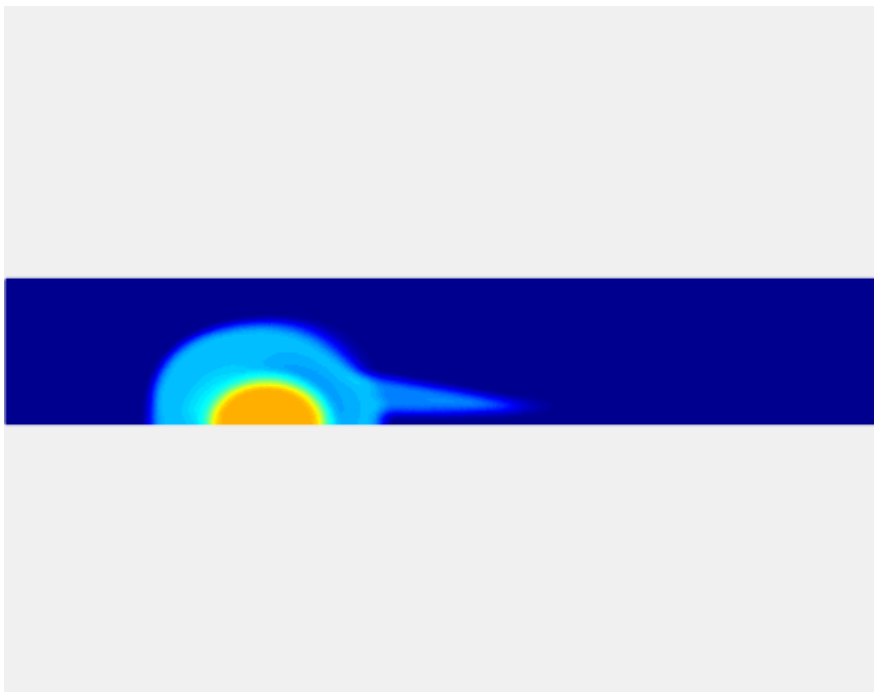
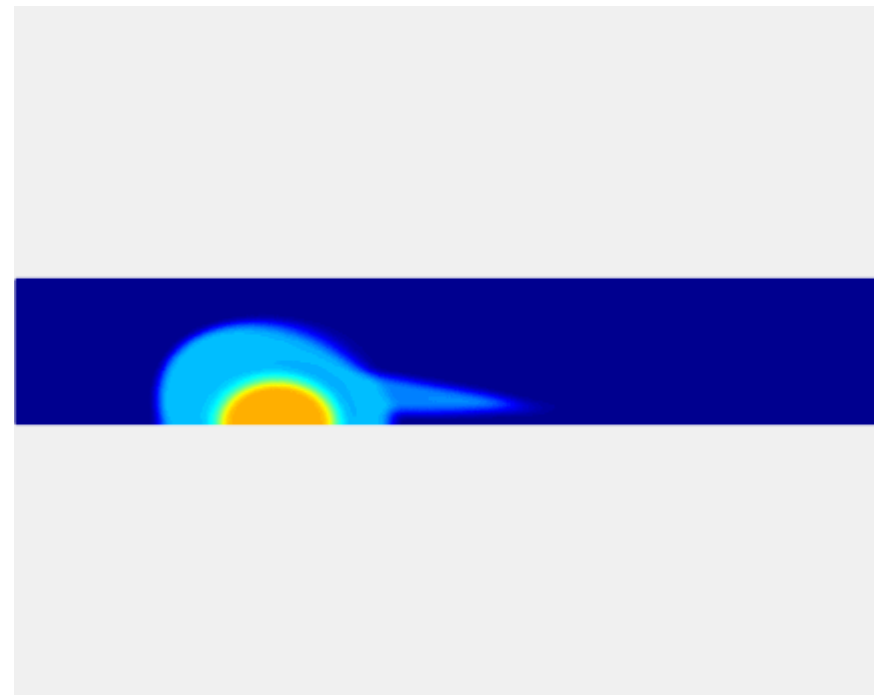
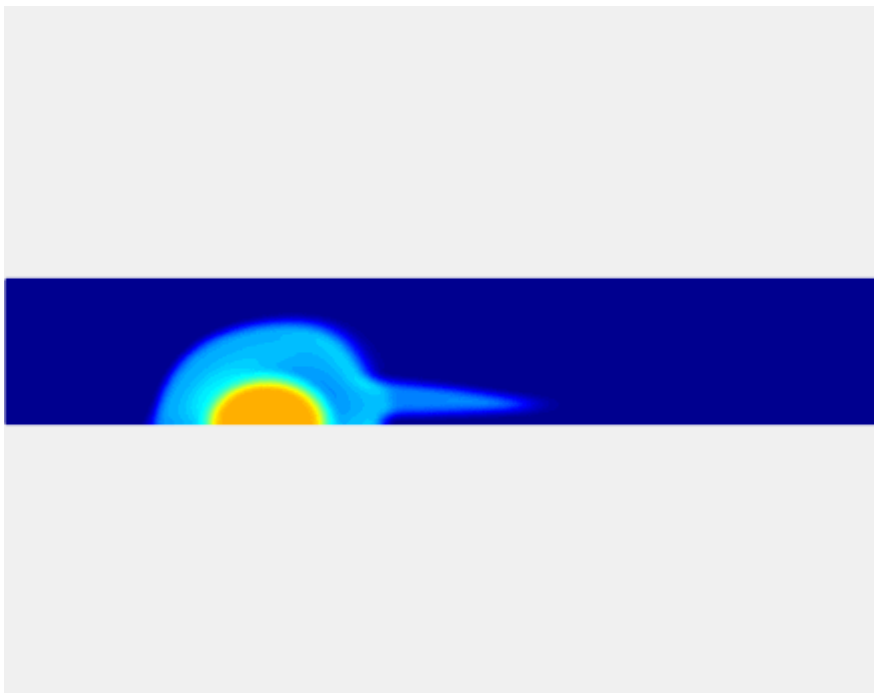


Figure 7. (a) Changes in clot shell porosity with flow shear rate. Inset indicates time-dependent variations in clot porosity at the shear rate of $1000 s^{-1}$. Here, macroscale deformation of a clot is almost not noticeable at $t = 0.2$ s. (b) Time-dependent changes of the maximum local wall shear rate assessed on the vessel wall opposite to the clot for different inlet shear rates. The Inset contains schematic diagram of wall shear rate. The clot shell permeability is $K_s = 10^{-12} m^2$. The shell porosity is the volume average of the porosity $(1 - \phi_3)$ in the shell region. ϕ_3 is redistributed due to the compression and shear (figure 5). Simulation show that the volume average of the clot in the shell region increases due to the platelets moving along the direction of the flow. (Online version in colour.)



Snapshots of surface of blood clot structure with different permeability and porosity. (a-b) $\Phi_0 = 0.7, K_S = 10^{-11} m^2, t = 0.1s, 0.2s$. (c-d) $\Phi_0 = 0.7, K_S = 10^{-12} m^2, t = 0.1s, 0.2s$. (e-f) $\Phi_0 = 0.5, K_S = 10^{-11} m^2, t = 0.1s, 0.2s$.

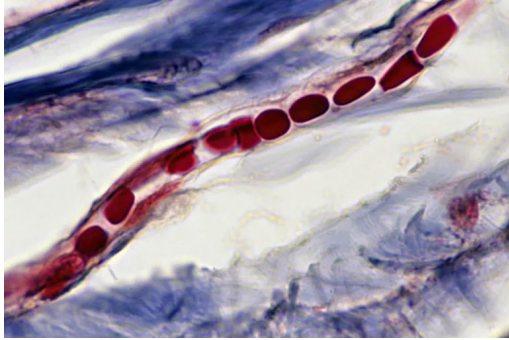
π



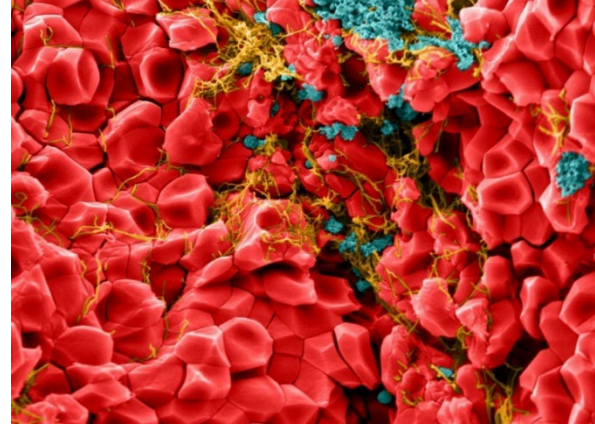
Movies show deformation of the clot at various permeabilities: $10^{(-11)}$ m², $10^{(-12)}$ m² and $10^{(-13)}$ m².

Blood Cells/Vesicles

π



<https://www.thoughtco.com/capillary-anatomy-373239>

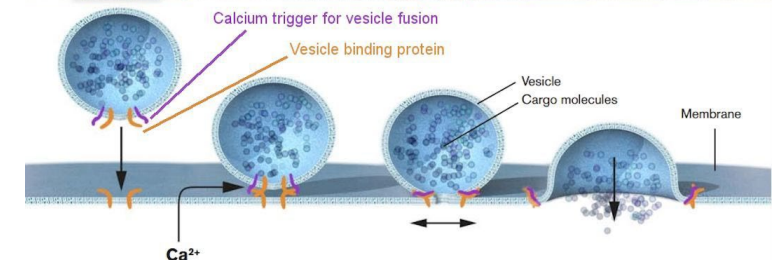
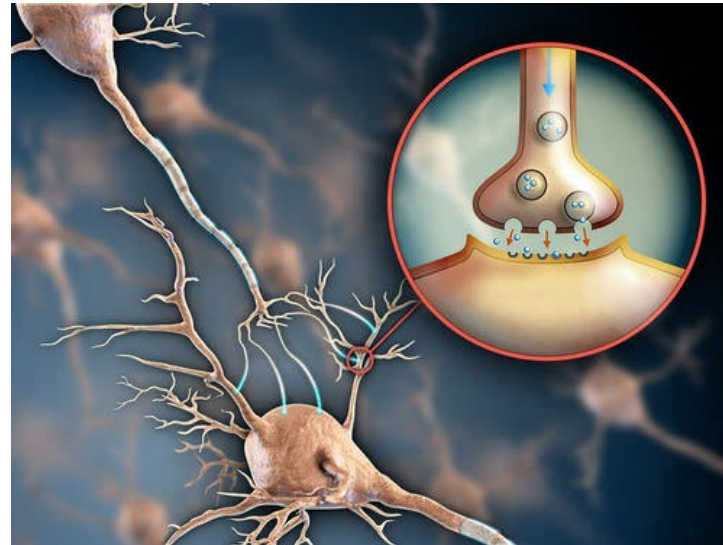
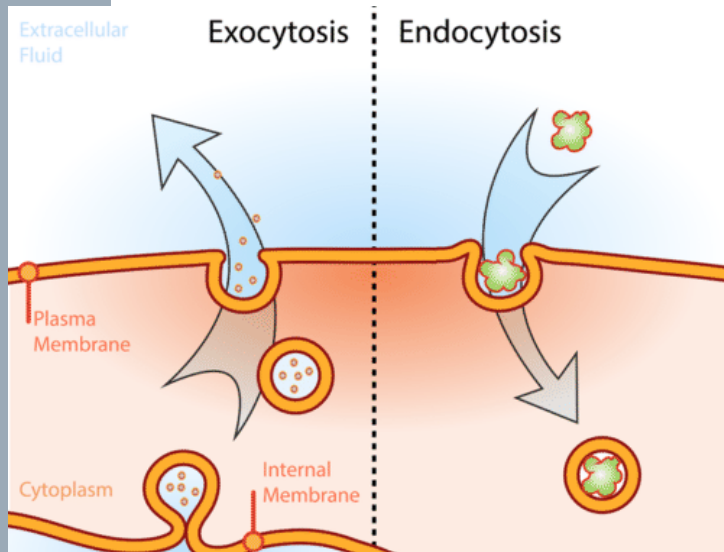


Blood. 123:10, 1596–1603. 2014;

- › **Dissipative Particle Dynamics:** Igor V Pivkin, George Em Karniadakis, Huan Lei, ...
- › **Immersed Boundary Method:** Charles S. Peskin, Ming-chih Lai, Huaxiong Huang, Yunchang Seol, James Feng
- › **Level Set Method:** Weiqing Ren, David Salac, Axel Voigt, Liu Yang, Qi Wang
- › **Phase Field Method:** Qiang Du, Chun Liu, Xiaoqiang Wang, Qi Wang, John S Lowengrub, Axel Voigt, Hao Wu...

Vesicles

- › Vesicles are fluid-filled sacs bounded by a closed lipid bilayer membrane. Vesicles play a critical role in intracellular transport of molecules and proteins

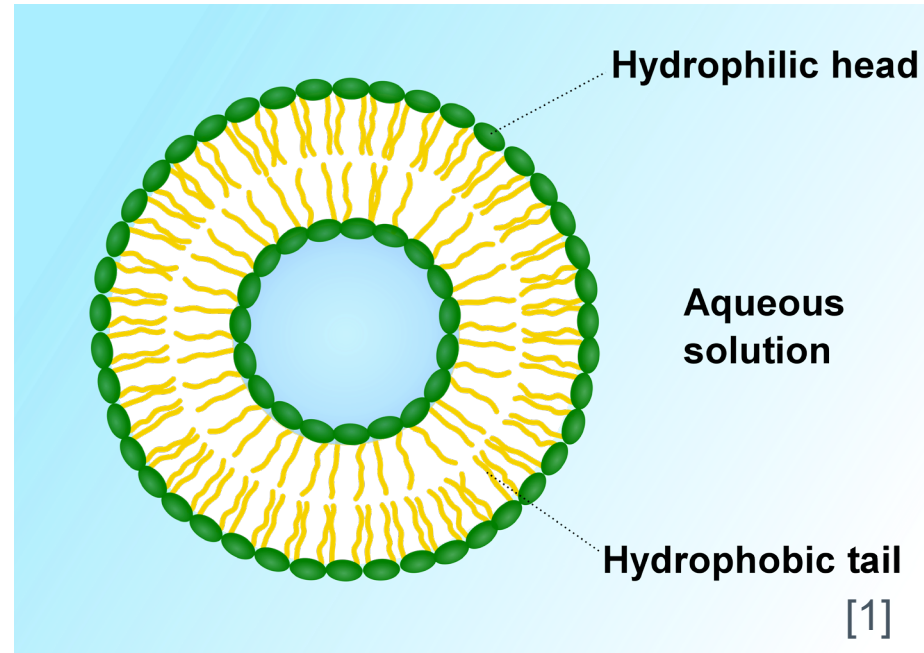


James E. Rothman

Randy W. Schekman Thomas C. Südhof

2013 Nobel Prize in Physiology or Medicine

Biological membrane



characteristics {
global inextensibility
local inextensibility } **surface conservation**
mass conservation

[1] [https://en.wikipedia.org/wiki/Vesicle_\(biology_and_chemistry\)#/media/File:Liposome_scheme-en.svg](https://en.wikipedia.org/wiki/Vesicle_(biology_and_chemistry)#/media/File:Liposome_scheme-en.svg)

(Energy) Variational Method

π

- **Step1:** Define energetic functional E^{tot} and dissipative functional Δ ;
- **Step2:** Kinematic assumptions: Laws of conservation with some unknown terms, for example flux, tensor;
- **Step3:** Taking the time derivative of the energetic functional and combining with the kinematic assumptions, get the form of $\frac{d}{dt} E^{tot}$;
- **Step4:** Comparing with $\frac{d}{dt} E^{tot}$ and dissipative functional Δ yields the expressions of unknown terms.



FIG. 1. A case of the phase definition of wall and vesicle. In the figure, we plot the value of $\phi + \phi_w$. In our model, ϕ is 1 and -1 in and outside the vesicle while ϕ_w is 0 on the wall and -1 at the edge in the domain. The wall and vesicle phases are defined by tanh function. The thickness of the wall phase is equal to the vesicle membrane. Here, ϕ and ϕ_w are slightly overlapping which means the attraction force is induced in the overlapping region.

Vesicle Model Derivation

The total energy is defined as:

$$E_{total} = \underbrace{E_{kin}}_{\text{Macroscale}} + \underbrace{E_{cell} + E_w}_{\text{Microscale}}$$

$$E_{kin} = \int_{\Omega} \left(\frac{1}{2} \rho |\mathbf{u}|^2 \right) dx$$

$$E_{cell} = E_{bend} + \frac{M_v (V(\phi) - V(\phi_0))^2}{2 V(\phi_0)} + \frac{M_s (S(\phi) - S(\phi_0))^2}{2 S(\phi_0)}$$

$$E_{bend} = \int_{\Omega} \frac{\hat{\kappa}_B}{2\gamma} \left| \frac{f(\phi)}{\gamma} \right|^2 dx$$

$$E_w = \sigma \int_{\partial\Omega_w} f_w(\phi) ds$$

Define the dissipation of energy:

$$\begin{aligned} \Delta = & \int_{\Omega} 2\eta |\mathbf{D}_{\eta}|^2 dx + \int_{\Omega} \frac{1}{M_{\phi}} |q_{\phi}|^2 dx + \int_{\Omega} \xi |\gamma \phi \nabla \lambda|^2 dx + \int_{\partial\Omega_w} \beta_s |\mathbf{u}_{\tau}|^2 ds \\ & + \int_{\partial\Omega_w} \kappa_{\Gamma} |J_{\Gamma}|^2 ds . \end{aligned}$$

M_v and M_s are global cell volume and surface area constrain coefficients

Wu, Hao, and Xiang Xu. "Global regularity, and stability of a hydrodynamic system modeling vesicle and fluid interactions." *SIAM Journal on Mathematical Analysis* 45.1 (2013): 181-214.

$$\begin{aligned} f(\phi) &= \frac{\delta G}{\delta \phi} = -\gamma^2 \Delta \phi + (\phi^2 - 1)\phi \\ G(\phi) &= \frac{\gamma^2 |\nabla \phi|^2}{2} + \frac{(1 - \phi^2)^2}{4} \\ S(\phi) &= \int_{\Omega} \frac{G(\phi)}{\gamma} \\ V(\phi) &= \int_{\Omega} \phi dx \\ f_w(\phi) &= \frac{Q_w}{4} (\phi^2 - 1)^2 (\phi_w^2 - 1) \end{aligned}$$

π

Begin with kinematic assumptions of the system:

$$\mathcal{P} \text{ is } (I - \mathbf{n}_m \otimes \mathbf{n}_m)$$

$$\mathbf{n}_m = \frac{\nabla \phi}{|\nabla \phi|}$$

$$\left\{ \begin{array}{l} \frac{\partial \phi}{\partial t} + \nabla \cdot (\mathbf{u} \phi) = q_\phi, \\ \rho \left(\frac{\partial \mathbf{u}}{\partial t} + (\mathbf{u} \cdot \nabla) \mathbf{u} \right) = \nabla \cdot \boldsymbol{\sigma}_\eta + \mathbf{F}_\phi, \\ \nabla \cdot \mathbf{u} = 0, \\ \delta_\gamma (\mathcal{P} : \nabla \mathbf{u}) + \xi \gamma^2 \nabla \cdot (\phi^2 \nabla \lambda) = 0. \end{array} \right.$$



$$F(u, \phi, P, \mu, \lambda, f)$$

Equations of **velocity, phase, pressure, chemical potential, local inextensibility, curvature**

Boundary conditions:

Voigt et al. J.C.P. 277(2014)

$$\left\{ \begin{array}{l} \mathbf{u} \cdot \mathbf{n} = 0, \\ \mathbf{u}_\tau \cdot \boldsymbol{\tau}_i = f_{\tau_i}, \\ \dot{\phi} = \frac{\partial \phi}{\partial t} + \mathbf{u} \cdot \nabla_\Gamma \phi = J_\Gamma \\ f = 0, \\ \partial_n \lambda = 0, \end{array} \right.$$

where q_ϕ is phase fields phenomenological term, $\boldsymbol{\sigma}_\eta$ is fluid shear stress, \mathbf{F}_ϕ is the cell membrane force acting on the fluid

$$\begin{aligned} \Delta &= \int_{\Omega} 2\eta |\mathbf{D}_{\eta}|^2 d\mathbf{x} + \int_{\Omega} \frac{1}{M_{\phi}} |q_{\phi}|^2 d\mathbf{x} + \int_{\partial\Omega_w} \beta_s |\mathbf{u}_{\tau}|^2 + \int_{\partial\Omega_w} \kappa_{\Gamma} |J_{\Gamma}|^2 dS, \\ \frac{d}{dt} E_{total} &= - \int_{\Omega} ((\boldsymbol{\sigma}_{\eta} + pI) : \nabla \mathbf{u}) d\mathbf{x} + \int_{\Omega} (\mathbf{F}_{\phi} - \mu \nabla \phi - \nabla \cdot (\lambda \delta \mathcal{P})) \cdot \mathbf{u} d\mathbf{x} + \int_{\Omega} \mu q_{\phi} d\mathbf{x} \\ &\quad + \int_{\partial\Omega_w} ((\boldsymbol{\sigma}_{\eta} + \lambda \delta \mathcal{P}) \cdot \mathbf{n}) \cdot \mathbf{u}_{\tau} dS + \int_{\partial\Omega_s} \hat{L}(\phi) \frac{\partial \phi}{\partial t} \\ &= - \int_{\Omega} ((\boldsymbol{\sigma}_{\eta} + pI) : \nabla \mathbf{u}) d\mathbf{x} + \int_{\Omega} (\mathbf{F}_{\phi} - \mu \nabla \phi - \nabla \cdot (\lambda \delta_{\epsilon} \mathcal{P})) \cdot \mathbf{u} d\mathbf{x} + \int_{\Omega} \mu q_{\phi} d\mathbf{x} \\ &\quad + \int_{\partial\Omega_w} ((\boldsymbol{\sigma}_{\eta} + \lambda \delta(\phi) \mathcal{P}) \cdot \mathbf{n}) \cdot \mathbf{u}_{\tau} dS + \int_{\partial\Omega_s} \hat{L}(\phi) (-\mathbf{u} \cdot \nabla_{\Gamma} \phi + J_{\Gamma}) \\ &= - \int_{\Omega} ((\boldsymbol{\sigma}_{\eta} + pI) : \nabla \mathbf{u}) d\mathbf{x} + \int_{\Omega} (\mathbf{F}_{\phi} - \mu \nabla \phi - \nabla \cdot (\lambda \delta \mathcal{P})) \cdot \mathbf{u} d\mathbf{x} + \int_{\Omega} \mu q_{\phi} d\mathbf{x} \\ &\quad + \int_{\partial\Omega_w} ((\boldsymbol{\sigma}_{\eta} + \lambda \delta \mathcal{P}) \cdot \mathbf{n} - \hat{L}(\phi) \nabla_{\Gamma} \phi) \cdot \mathbf{u}_{\tau} dS + \int_{\partial\Omega_w} \hat{L}(\phi) J_{\Gamma} dS, \end{aligned}$$

compare the corresponding terms



$$\begin{cases} \boldsymbol{\sigma}_{\eta} = 2\eta \mathbf{D}_{\eta} - pI, & \text{in } \Omega, \\ q_{\phi} = -M_{\phi} \mu, & \text{in } \Omega, \\ \mathbf{F}_{\phi} = \mu \nabla \phi + \nabla \cdot (\lambda \delta \mathcal{P}), & \text{in } \Omega, \\ J_{\Gamma} = -\kappa_{\Gamma}^{-1} \hat{L}(\phi), & \text{on } \partial\Omega_w, \\ u_{\tau_i} = \beta_{\Gamma}^{-1} (-(\mathbf{n} \cdot (\boldsymbol{\sigma}_{\eta} + \lambda \delta_{\epsilon} \mathcal{P}) \cdot \boldsymbol{\tau}_i) + \hat{L}(\phi) \partial_{\tau_i} \phi), i = 1, 2, & \text{on } \partial\Omega_w \end{cases}$$

$$\left\{ \begin{array}{l} \frac{\partial \phi}{\partial t} + \nabla \cdot (\mathbf{u}\phi) = -M_\phi \mu , \\ \mu = \frac{\hat{\kappa}_B}{\gamma^3} g(\phi) + M_v \frac{V(\phi) - V(\phi_0)}{V(\phi_0)} + \frac{M_s}{\gamma} \frac{S(\phi) - S(\phi_0)}{S(\phi_0)} f(\phi) + \frac{\partial f_w}{\partial \phi} , \\ g(\phi) = -\gamma^2 \Delta f + (3\phi^2 - 1)f(\phi), \\ f(\phi) = -\gamma^2 \Delta \phi + (\phi^2 - 1)\phi , \\ \rho \left(\frac{\partial \mathbf{u}}{\partial t} + (\mathbf{u} \cdot \nabla) \mathbf{u} \right) + \nabla p = \nabla \cdot (2\eta \mathbf{D}_\eta) + \mu \nabla \phi + \nabla \cdot (\lambda \delta_\gamma \mathcal{P}) , \\ \nabla \cdot \mathbf{u} = 0 , \\ \delta_\gamma (\mathcal{P} : \nabla \mathbf{u}) + \xi \gamma^2 \nabla \cdot (\phi^2 \nabla \lambda) = 0 , \end{array} \right.$$

$$\left\{ \begin{array}{l} \mathbf{u} \cdot \mathbf{n} = 0 , \\ -\beta_s u_{\tau_i} = (\mathbf{n} \cdot (\boldsymbol{\sigma}_\eta + \lambda \delta_\gamma \mathcal{P}) \cdot \boldsymbol{\tau}_i) - \hat{L}(\phi) \partial_{\tau_i} \phi , \quad i = 1, 2, \\ f = 0 , \\ \kappa_\Gamma \left(\frac{\partial \phi}{\partial t} + \mathbf{u} \cdot \nabla_\Gamma \phi \right) = -\hat{L}(\phi) , \\ \hat{L}(\phi) = \frac{\hat{\kappa}_B}{\gamma} \partial_n f + M_s \frac{S(\phi) - S(\phi_0)}{S(\phi_0)} \gamma \partial_n \phi , \\ \partial_n \lambda = 0 . \end{array} \right.$$

Dimensionless Eqs. & Energy Dissipation Law

$$\left\{ \begin{array}{ll}
 Re\left(\frac{\partial \mathbf{u}}{\partial t} + (\mathbf{u} \cdot \nabla) \mathbf{u}\right) + \nabla P = \nabla \cdot (2\eta \mathbf{D}) + \mu \nabla \phi + \nabla \cdot (\lambda \delta_\epsilon \mathcal{P}), & \text{in } \Omega \\
 \nabla \cdot \mathbf{u} = 0, & \text{in } \Omega \\
 \frac{\partial \phi}{\partial t} + \mathbf{u} \cdot \nabla \phi = -\mathcal{M} \mu, & \text{in } \Omega \\
 \mu = \kappa_B g(\phi) + \mathcal{M}_v \frac{(V(\phi) - V(\phi_0))}{V(\phi_0)} + \mathcal{M}_s \frac{(S(\phi) - S(\phi_0))}{S(\phi_0)} f(\phi) + \alpha_w \frac{\partial f_w}{\partial \phi}, & \text{in } \Omega \\
 f(\phi) = -\epsilon \Delta \phi + \frac{(\phi^2 - 1)}{\epsilon} \phi, \quad g(\phi) = -\Delta f + \frac{1}{\epsilon^2} (3\phi^2 - 1) f(\phi), & \text{in } \Omega \\
 \delta_\epsilon (\mathcal{P} : \nabla \mathbf{u}) + \xi \epsilon^2 \nabla \cdot (\phi^2 \nabla \lambda) = 0, & \text{in } \Omega
 \end{array} \right. \quad \begin{array}{l}
 V(\phi) = \int_\Omega \phi d\mathbf{x} \\
 S(\phi) = \int_\Omega \frac{\epsilon}{2} |\nabla \phi|^2 + \frac{1}{4\epsilon} (\phi^2 - 1)^2 d\mathbf{x}
 \end{array}$$

Boundary condition:

$$\left\{ \begin{array}{ll}
 \kappa \dot{\phi} + L(\phi) = 0, & \text{on } \partial\Omega_w \\
 L(\phi) = \kappa_B \partial_n f + \epsilon \mathcal{M}_s \frac{S(\phi) - S(\phi_0)}{S(\phi_0)} \partial_n \phi, & \text{on } \partial\Omega_w \\
 -l_s^{-1} u_{\tau_i} = \boldsymbol{\tau}_i \cdot (2\eta \mathbf{D}_\eta + \lambda \delta_\epsilon \mathcal{P}) \cdot \mathbf{n} - L(\phi) \partial_{\tau_i} \phi, \quad i = 1, 2, & \text{on } \partial\Omega_w \\
 f = 0, & \text{on } \partial\Omega_w \\
 \partial_n \lambda = 0, & \text{on } \partial\Omega_w
 \end{array} \right.$$

Here dimensionless constants $\epsilon = \frac{\gamma}{L}$, $Re = \frac{\rho_0 U L}{\eta_0}$, $\mathcal{M} = M \eta_0$, $\kappa_B = \frac{\hat{\kappa}}{L^2 \eta_0 U}$, $k = \frac{\hat{k}}{\eta_0 L}$,
 $l_s = \frac{\eta_0}{\beta_s L}$, $\alpha_w = \frac{\sigma}{\eta_0 U}$, $\mathcal{M}_f = \frac{M_s}{\eta_0 U}$, $\mathcal{M}_v = \frac{M_v L}{\eta_0 U}$.

$$\begin{aligned}\frac{d}{dt}\mathcal{E}_{total} &= \frac{d}{dt}(\mathcal{E}_{kin} + \mathcal{E}_{cell} + \mathcal{E}_w) \\ &= -2\|\eta^{1/2}\mathbf{D}_\eta\|^2 - \mathcal{M}\|\mu\|^2 - \kappa\|\dot{\phi}\|_w^2 - \|l_s^{-1/2}\mathbf{u}_\tau\|_w^2,\end{aligned}$$

where $\mathcal{E}_{total} = \mathcal{E}_{kin} + \mathcal{E}_{cell} + \mathcal{E}_w$, $\mathcal{E}_{kin} = \frac{1}{2}\|\mathbf{u}\|^2$, $\mathcal{E}_{cell} = \frac{\kappa_B\|f\|^2}{2\epsilon} + \mathcal{M}_v\frac{(V(\phi)-V(\phi_0))^2}{2V(\phi_0)} + \mathcal{M}_s\frac{(S(\phi)-S(\phi_0))^2}{2S(\phi_0)}$

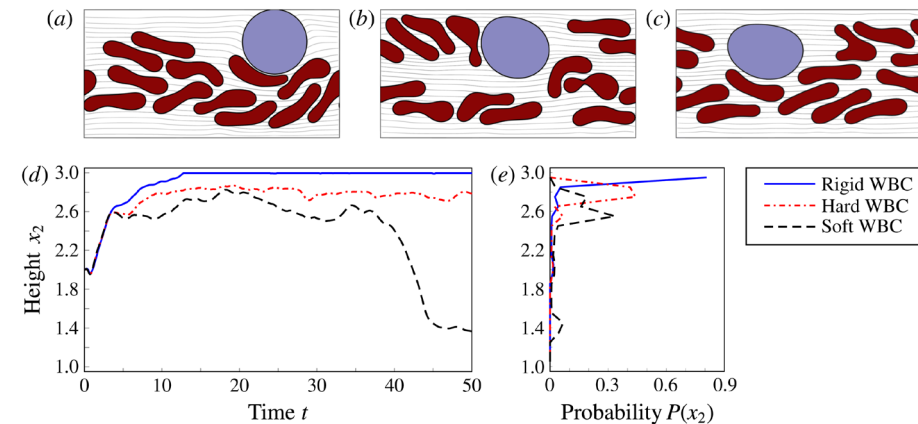
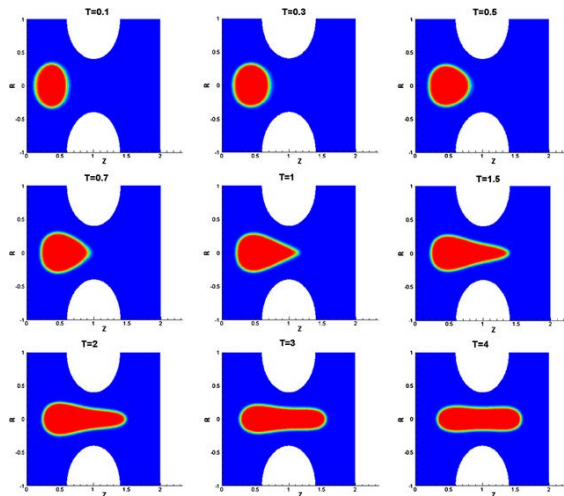
and $\mathcal{E}_w = \alpha_w \int_w f_w ds$.

Numerical Scheme

π

› Existing Method

- Qiang Du & Xiaoqiang Wang et al.: Euler Method
- John S Lowengrub & Axel Voigt et al.: Adaptive time step
- R. Chen & X.F Yang, F Guillén-González & G Tierra: Decoupled energy stable scheme



R. Chen and X.F Yang Journal of Computational Physics 302:509-523

Wieland Marth, Sebastian Aland, and Axel Voigt, Journal of Fluid Mechanics 790

Discrete Scheme and Energy Law

$$\left\{ \begin{aligned} & \frac{\mathbf{u}^{n+1} - \mathbf{u}^n}{\Delta t} + (\mathbf{u}^{n+\frac{1}{2}} \cdot \nabla) \mathbf{u}^{n+\frac{1}{2}} + \frac{1}{Re} \nabla P^{n+\frac{1}{2}} = \frac{1}{Re} \nabla \cdot (\eta^n (\nabla \mathbf{u}^{n+\frac{1}{2}} + (\nabla \mathbf{u}^{n+\frac{1}{2}})^T)) \\ & \quad + \frac{1}{Re} \mu^{n+\frac{1}{2}} \nabla \phi^{n+\frac{1}{2}} + \frac{1}{Re} \nabla \cdot (\lambda^{n+\frac{1}{2}} \mathcal{P}^n \delta_\epsilon) , \\ & \nabla \cdot \mathbf{u}^{n+\frac{1}{2}} = 0 , \\ & \frac{\phi^{n+1} - \phi^n}{\Delta t} + (\mathbf{u}^{n+\frac{1}{2}} \cdot \nabla) \phi^{n+\frac{1}{2}} = -\mathcal{M} \mu^{n+\frac{1}{2}} , \\ & \mu^{n+\frac{1}{2}} = \kappa_B g(\phi^{n+1}, \phi^n) + \mathcal{M}_v \frac{(V(\phi^{n+\frac{1}{2}}) - V(\phi_0))}{V(\phi_0)} \\ & \quad + \mathcal{M}_s \frac{(S(\phi^{n+\frac{1}{2}}) - S(\phi_0))}{S(G_0)} f(\phi^{n+1}, \phi^n) + \alpha_w \frac{f_w^{n+1} - f_w^n}{\phi^{n+1} - \phi^n} , \\ & f^{n+\frac{1}{2}} = -\epsilon \Delta \phi^{n+\frac{1}{2}} + \frac{1}{\epsilon} ((\phi^{n+\frac{1}{2}})^2 - 1) \phi^{n+\frac{1}{2}} , \\ & \xi \epsilon^2 \nabla \cdot ((\phi^n)^2 \nabla \lambda^{n+\frac{1}{2}}) + \delta_\epsilon \mathcal{P}^n : \nabla \mathbf{u}^{n+\frac{1}{2}} = 0 . \end{aligned} \right.$$

$$\left\{ \begin{aligned} & \kappa \dot{\phi}^{n+\frac{1}{2}} = -L^{n+\frac{1}{2}} , \\ & L^{n+\frac{1}{2}} = \kappa_B \partial_n f^{n+\frac{1}{2}} + \mathcal{M}_s \epsilon \frac{S(\phi^{n+\frac{1}{2}}) - S_0}{S_0} \partial_n \phi^{n+\frac{1}{2}} , \\ & -l_s^{-1} u_{\tau_i}^{n+\frac{1}{2}} = \boldsymbol{\tau}_i \cdot (\eta^n (\nabla \mathbf{u}^{n+\frac{1}{2}} + (\nabla \mathbf{u}^{n+\frac{1}{2}})^T) + \lambda^{n+\frac{1}{2}} \delta_\epsilon \mathcal{P}^n) \cdot \mathbf{n} \\ & \quad - L^{n+\frac{1}{2}} \partial_{\tau_i} \phi^{n+\frac{1}{2}} , \quad i = 1, 2, \\ & f^{n+\frac{1}{2}} = 0 , \\ & \partial_n \lambda^{n+\frac{1}{2}} = 0 , \end{aligned} \right.$$

$$(\cdot)^{n+\frac{1}{2}} = \frac{(\cdot)^n + (\cdot)^{n+1}}{2}$$

$$\mathcal{P}^n = I - \mathbf{n}_m^n \otimes \mathbf{n}_m^n$$

$$\mathbf{n}_m^n = \frac{\nabla \phi^n}{|\nabla \phi^n|}$$

$$f(\phi^{n+1}, \phi^n) = -\epsilon \Delta \phi^{n+\frac{1}{2}} + \frac{1}{4\epsilon} ((\phi^{n+1})^2 + (\phi^n)^2 - 2)(\phi^{n+1} + \phi^n)$$

$$g(\phi^{n+1}, \phi^n) = \left(-\Delta f^{n+\frac{1}{2}} + \frac{1}{\epsilon^2} ((\phi^{n+1})^2 + (\phi^n)^2 + \phi^{n+1} \phi^n - 1) f^{n+\frac{1}{2}} \right)$$

$$\begin{aligned}
 \mathcal{E}_{total}^{n+1} - \mathcal{E}_{total}^n &= (\mathcal{E}_{kin}^{n+1} + \mathcal{E}_{cell}^{n+1} + \mathcal{E}_w^{n+1}) - (\mathcal{E}_{kin}^n + \mathcal{E}_{cell}^n + \mathcal{E}_w^n) \\
 &= \Delta t \left(-2\|(\eta^n)^{1/2} \mathbf{D}_\eta^{n+\frac{1}{2}}\|^2 - \mathcal{M}\|\mu^{n+\frac{1}{2}}\|^2 - \xi\|\epsilon\phi^n \nabla \lambda^{n+\frac{1}{2}}\|^2 \right. \\
 &\quad \left. - \frac{1}{\kappa} \|L(\phi^{n+\frac{1}{2}})\|_w^2 - \|l_s^{-1/2} \mathbf{u}_\tau^{n+\frac{1}{2}}\|_w^2 \right),
 \end{aligned}$$

where $\mathcal{E}_{total}^n = \mathcal{E}_{kin}^n + \mathcal{E}_{cell}^n + \mathcal{E}_w^n$ with $\mathcal{E}_{kin}^n = \frac{Re}{2} \|\mathbf{u}^n\|^2$, $\mathcal{E}_{cell}^n = \frac{\kappa_B \|f^n\|^2}{2\epsilon} + \mathcal{M}_v \frac{(V(\phi^n) - V(\phi_0))^2}{2V(\phi_0)} + \mathcal{M}_s \frac{(S(\phi^n) - S(\phi_0))^2}{2S(\phi_0)}$ and $\mathcal{E}_w^n = \alpha_w \int_{\partial\Omega_w} f_w^n ds$.

Fully-discrete C^0 finite element scheme

$$\int_{\Omega} \left(\frac{\mathbf{u}_h^{n+1} - \mathbf{u}_h^n}{\Delta t} + (\mathbf{u}_h^{n+\frac{1}{2}} \cdot \nabla) \mathbf{u}_h^{n+\frac{1}{2}} + \frac{1}{Re} \nabla P_h^{n+\frac{1}{2}} \right) \cdot \mathbf{v}_h = - \int_{\Omega} \frac{1}{Re} (\eta_h^n (\nabla \mathbf{u}_h^{n+\frac{1}{2}} + (\nabla \mathbf{u}_h^{n+\frac{1}{2}})^T)) : \nabla \mathbf{v}_h$$

$$+ \int_{\Omega} \frac{1}{Re} \mu_h^{n+\frac{1}{2}} \nabla \phi_h^{n+\frac{1}{2}} \cdot \mathbf{v}_h - \int_{\Omega} \frac{1}{Re} \lambda_h^{n+\frac{1}{2}} \mathcal{P}_h^n \delta_{\epsilon} : \mathbf{v}_h$$

$$+ \int_{\partial \Omega_w} \frac{1}{Re} \mathbf{n} \cdot (\eta_h^n (\nabla \mathbf{u}_h^{n+\frac{1}{2}} + (\nabla \mathbf{u}_h^{n+\frac{1}{2}})^T) + \lambda_h^{n+\frac{1}{2}} \mathcal{P}_h^n \delta_{\epsilon}) \cdot \mathbf{v}_h ,$$

$$\int_{\Omega} (\nabla \cdot \mathbf{u}_h^{n+\frac{1}{2}}) q_h = 0 ,$$

$$\int_{\Omega} \left(\frac{\phi_h^{n+1} - \phi_h^n}{\Delta t} + (\mathbf{u}_h^{n+\frac{1}{2}} \cdot \nabla) \phi_h^{n+\frac{1}{2}} \right) \psi_h = - \int_{\Omega} \mathcal{M} \mu_h^{n+\frac{1}{2}} \psi_h ,$$

$$\int_{\Omega} \mu_h^{n+\frac{1}{2}} \chi_h = \int_{\Omega} (\kappa_B \frac{1}{\epsilon^2} ((\phi_h^{n+1})^2 + (\phi_h^n)^2 + \phi_h^{n+1} \phi_h^n - 1) f_h^{n+\frac{1}{2}} + \mathcal{M}_v \frac{(V(\phi_h^{n+\frac{1}{2}}) - V(\phi_0))}{V(\phi_0)})$$

$$+ \mathcal{M}_s \frac{(S(\phi_h^{n+\frac{1}{2}}) - S(\phi_0))}{S(G_0)} \left(\frac{1}{4\epsilon} ((\phi_h^{n+1})^2 + (\phi_h^n)^2 - 2)(\phi_h^{n+1} + \phi_h^n) \right) \chi_h$$

$$+ \int_{\Omega} (\kappa_B \nabla f_h^{n+\frac{1}{2}} + \mathcal{M}_s \epsilon \frac{(S(\phi_h^{n+\frac{1}{2}}) - S(\phi_0))}{S(G_0)} \nabla \phi_h^{n+\frac{1}{2}}) \cdot \nabla \chi_h$$

$$- \int_{\partial \Omega_w} (\kappa_B \partial_{\mathbf{n}} f_h^{n+\frac{1}{2}} + \mathcal{M}_s \epsilon \frac{(S(\phi_h^{n+\frac{1}{2}}) - S(\phi_0))}{S(G_0)} \partial_{\mathbf{n}} \phi_h^{n+\frac{1}{2}}) \chi_h ,$$

$$\int_{\Omega} f_h^{n+\frac{1}{2}} \zeta_h = \int_{\Omega} \epsilon \nabla \phi_h^{n+\frac{1}{2}} \cdot \nabla \zeta_h + \int_{\Omega} \frac{1}{\epsilon} ((\phi_h^{n+\frac{1}{2}})^2 - 1) \phi_h^{n+\frac{1}{2}} \zeta_h - \int_{\partial \Omega_w} \epsilon \partial_{\mathbf{n}} \phi_h^{n+\frac{1}{2}} \zeta_h ,$$

$$- \int_{\Omega} \xi \epsilon^2 ((\phi_h^n)^2 \nabla \lambda_h^{n+\frac{1}{2}}) \cdot \nabla \Theta_h + \int_{\Omega} \delta_{\epsilon} \mathcal{P}_h^n : \nabla \mathbf{u}_h^{n+\frac{1}{2}} \Theta_h + \int_{\partial \Omega_w} \xi \epsilon^2 ((\phi_h^n)^2 \partial_{\mathbf{n}} \lambda_h^{n+\frac{1}{2}}) \Theta_h = 0 .$$

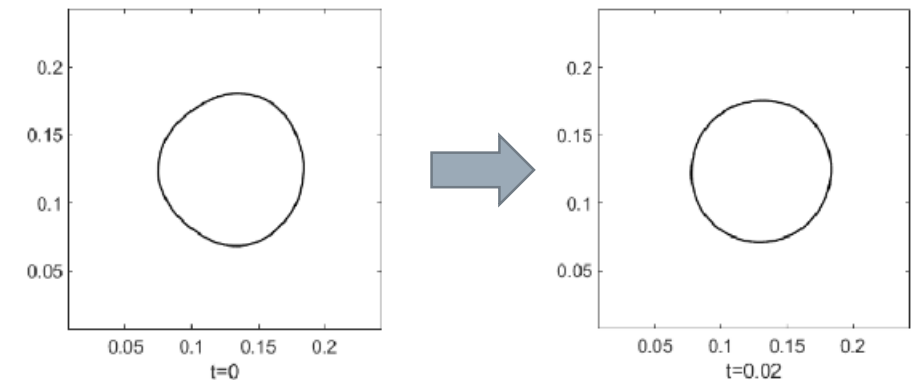
$$\mathcal{E}_{total,h}^{n+1} - \mathcal{E}_{total,h}^n = \frac{\Delta t}{Re} \left(-2 \|(\eta_h^n)^{1/2} \mathbf{D}_{\eta}^{n+\frac{1}{2}}\|^2 - \mathcal{M} \|\mu_h^{n+\frac{1}{2}}\|^2 - \xi \| \epsilon \phi_h^n \nabla \lambda_h^{n+\frac{1}{2}} \|^2 \right. \\ \left. - \frac{1}{\kappa} \|L(\phi_h^{n+\frac{1}{2}})\|_w^2 - \|l_s^{-1/2} \mathbf{u}_{\tau,h}^{n+\frac{1}{2}}\|_w^2 \right) ,$$

π Convergence study

reference: space: dh=1/240
time: dt=0.00004

Space step h	P2 Element					
	Err(u_x)	Rate	Err(u_y)	Rate	Err(c)	Rate
1/47	1.3e-1		1.5e-1		1.4e-2	
1/71	8.3e-2	1.15	7.6e-2	1.71	6.1e-3	1.97
1/107	3.8e-2	1.94	3.7e-2	1.83	2.3e-3	2.45
1/160	1.5e-2	2.35	1.3e-2	2.59	5.7e-4	3.42

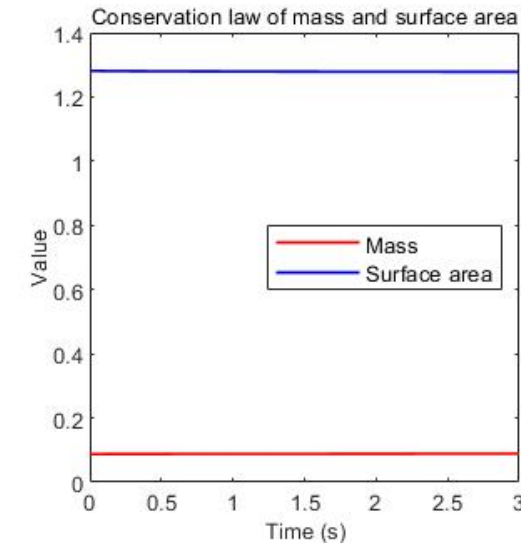
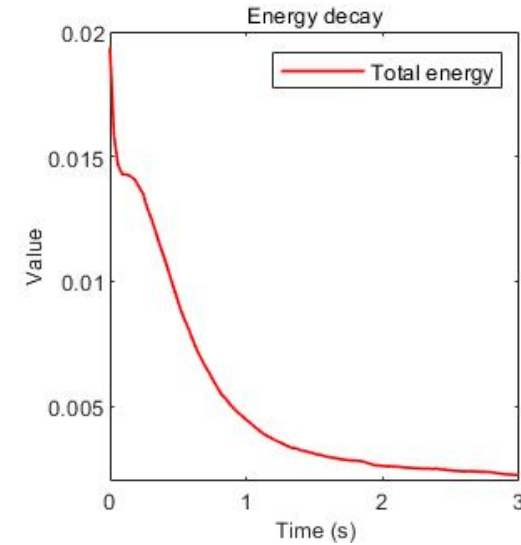
time step dt	P2 Element					
	Err(u_x)	Rate	Err(u_y)	Rate	Err(c)	Rate
0.0002025	1.0e-2		1.1e-2		2.1e-4	
0.000135	6.1e-3	1.31	6.2e-3	1.34	1.4e-4	1.06
0.00009	3.2e-3	1.57	3.2e-3	1.61	8.1e-5	1.32
0.00006	1.3e-3	2.26	1.3e-3	2.30	3.6e-5	2.01



$$Re = 2 \times 10^{-4}, \delta_\epsilon = |\nabla \phi^n|^2, \mathcal{M} = 5 \times 10^{-5}, \kappa_B = 8 \times 10^{-1}, \epsilon = 2.5 \times 10^{-2}, \mathcal{M}_v = 20, \mathcal{M}_s = 2, \xi = 1.6 \times 10^5, \kappa = 8 \times 10^{-10}, \alpha_w = 2 \times 10^9, l_s = 5 \times 10^{-3}.$$

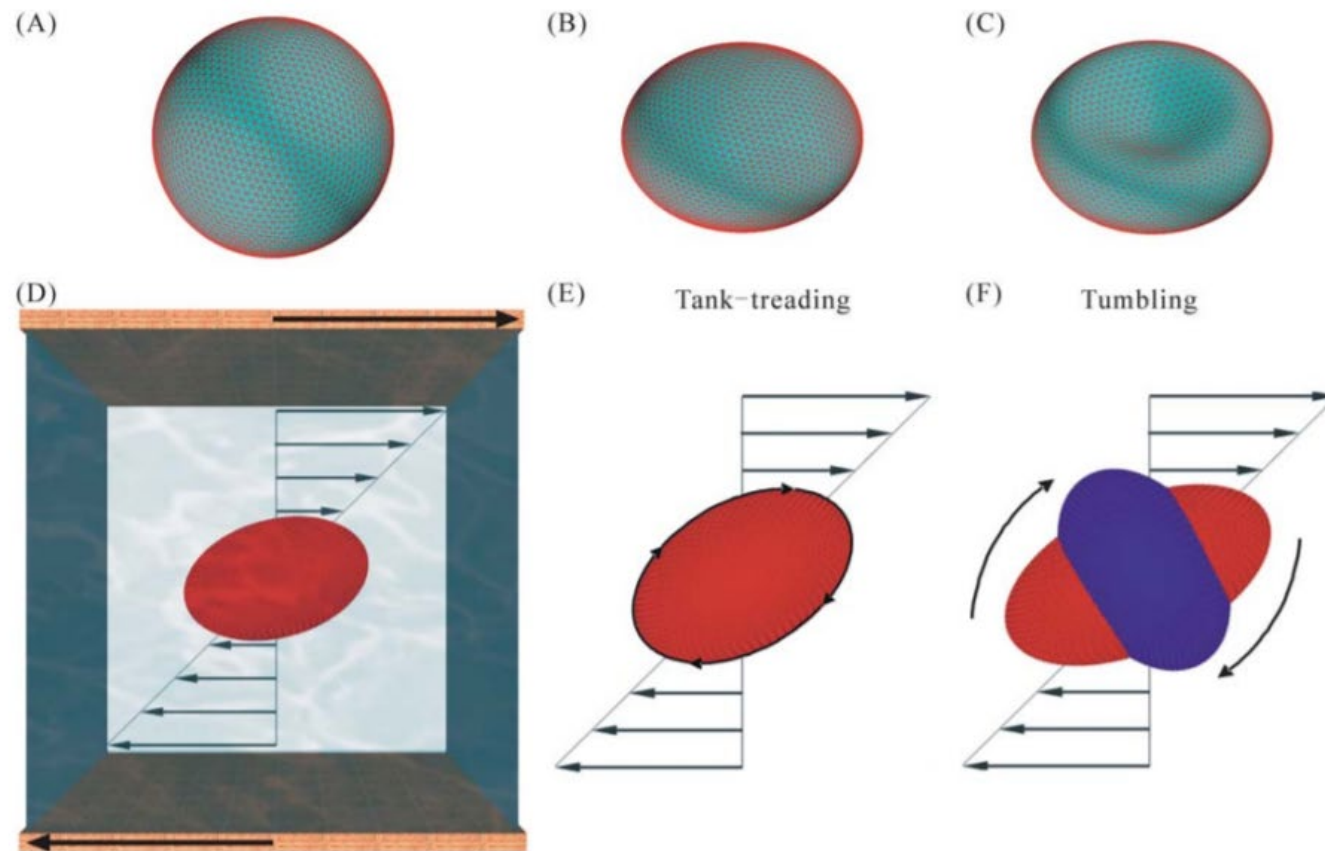
Conservation law and energy decaying law

π



$$Re = 2 \times 10^{-4}, \delta_\epsilon = 10 \times |\nabla\phi^n|^2, \mathcal{M} = 2.5 \times 10^{-3}, \kappa_B = 2, \epsilon = 7.5 \times 10^{-3}, \mathcal{M}_v = 20, \mathcal{M}_s = 2, \xi = 7.1 \times 10^4, \kappa = 2 \times 10^{-10}, \alpha_w = 2 \times 10^9, l_s = 0.5.$$

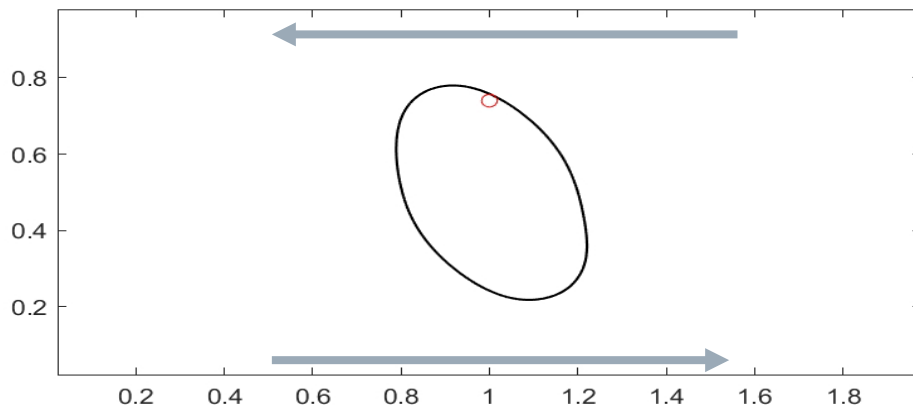
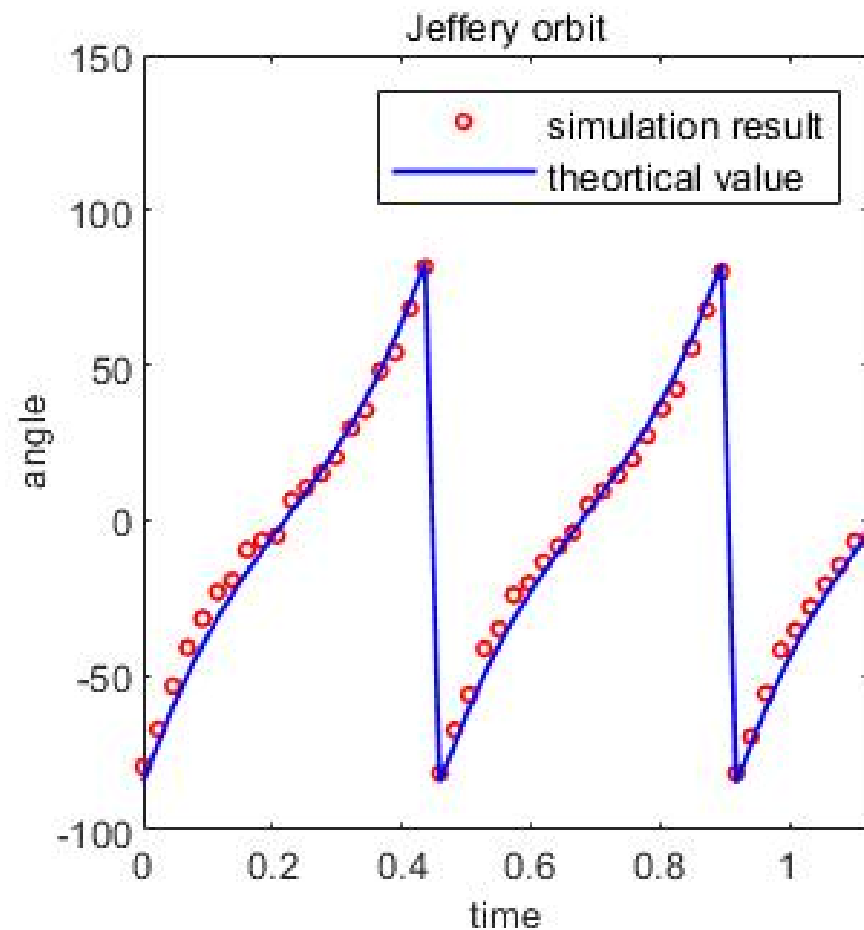
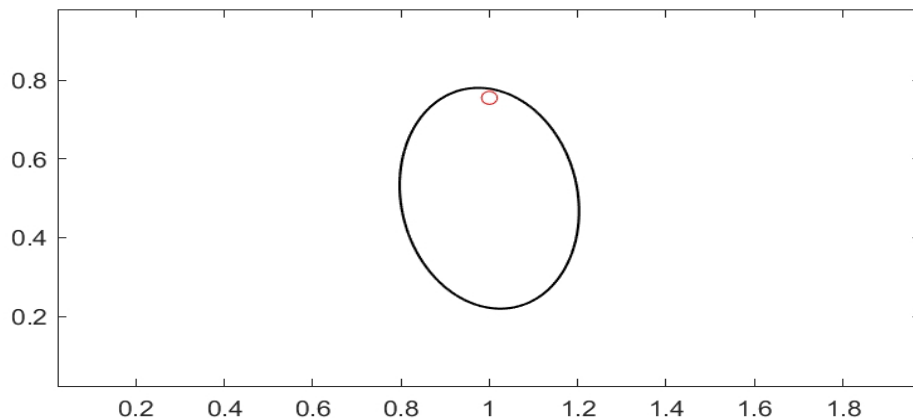
Tumbling and Tank Treading



Luo, Z. Y., Wang, S. Q., He, L., Xu, F., & Bai, B. F. (2013). Inertia-dependent dynamics of three-dimensional vesicles and red blood cells in shear flow. *Soft Matter*, 9(40), 9651-9660.

π

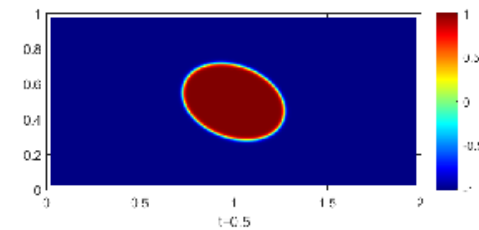
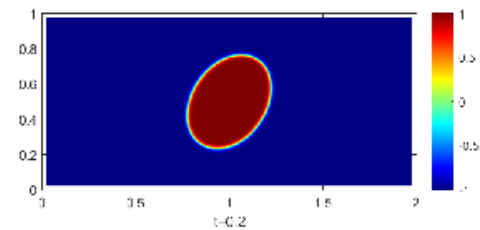
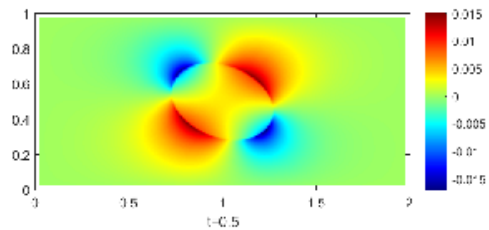
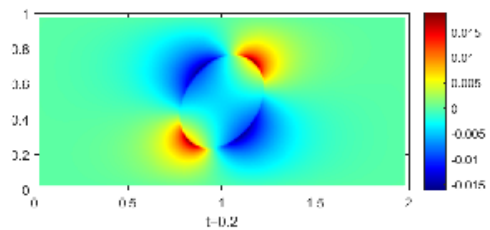
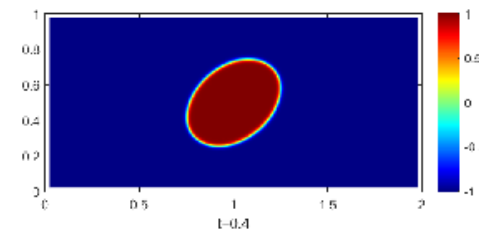
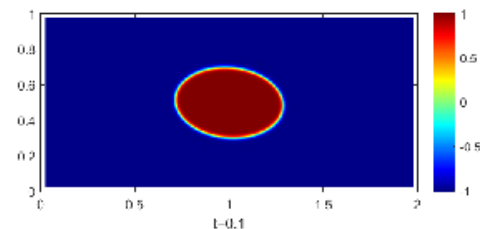
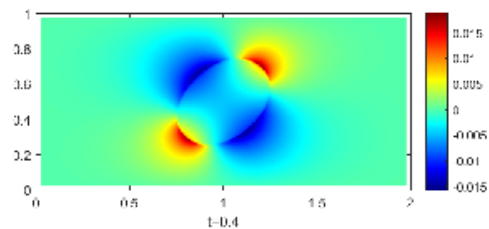
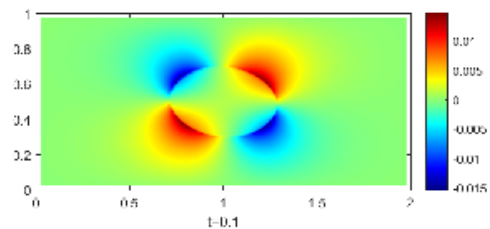
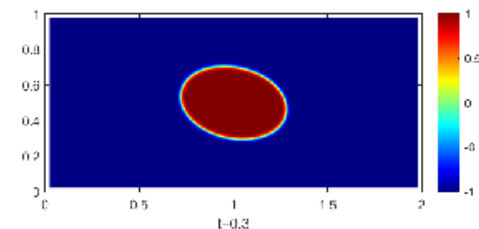
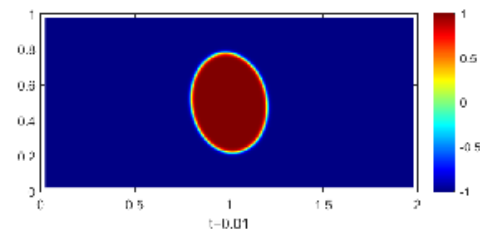
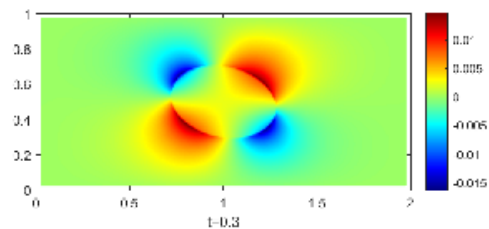
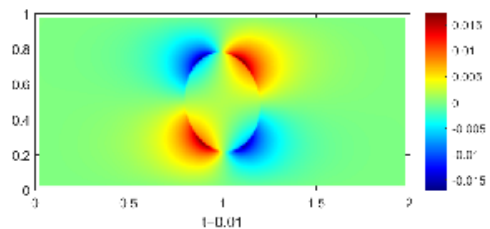
Tumbling and tank treading

 $\eta_{out} : \eta_{in} = 1:1$  $\eta_{out} : \eta_{in} = 1:500$ 

$Re = 2 \times 10^{-4}$, $\eta_{out} = 1$, $\eta_{in} = 500$, $\delta_\epsilon = |\nabla \phi^n|^2$, $\mathcal{M} = 10^{-3}$, $\kappa_B = 5 \times 10^{-3}$, $\epsilon = 7.5 \times 10^{-3}$, $\mathcal{M}_v = 20$, $\mathcal{M}_s = 200$, $\xi = 1.78 \times 10^7$, $\kappa = 2 \times 10^{-12}$, $\alpha_w = 2 \times 10^9$, $l_s = 0.2$. 51

π

Tumbling and tank treading



π

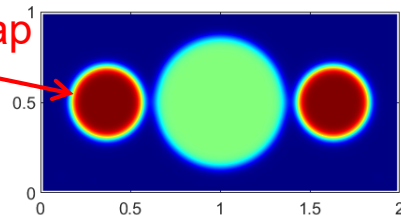
Nonlinear elastic and viscoelastic deformation with optical tweezers

experiment [1]

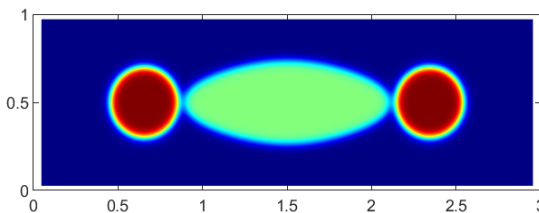
0 pN



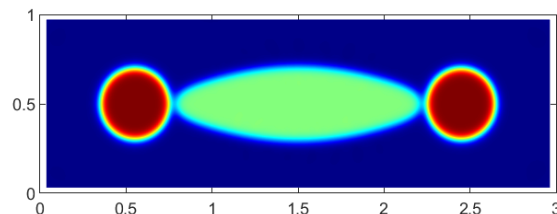
optical trap



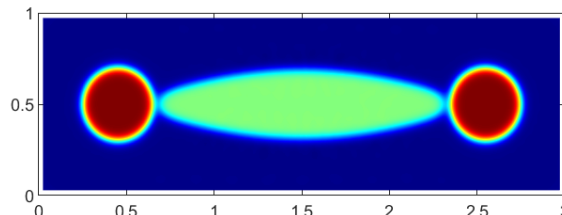
67 pN



130 pN



193 pN



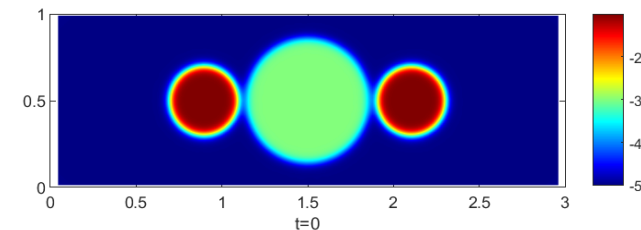
$$H_{trap} = -Q_{trap} (\phi_{trap}^2 - 1)(\phi^2 - 1)$$

0pN

65pN

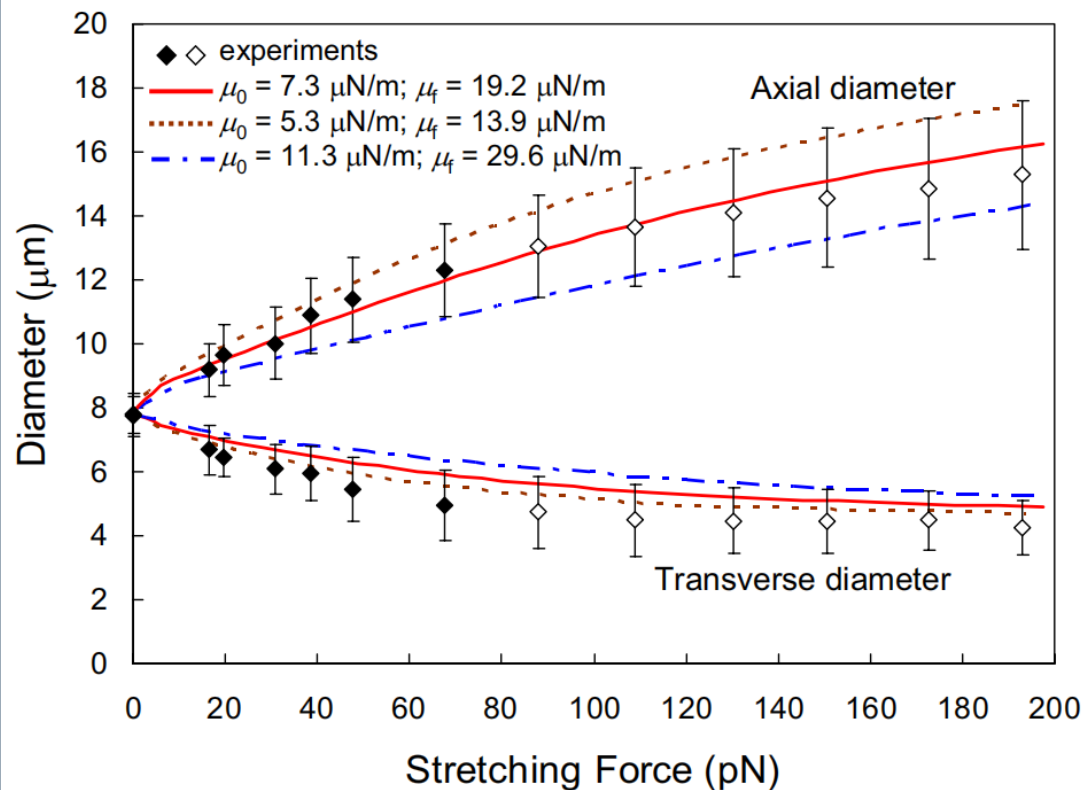
$$F = \frac{\partial H_w}{\partial \phi} \nabla \phi$$

130pN

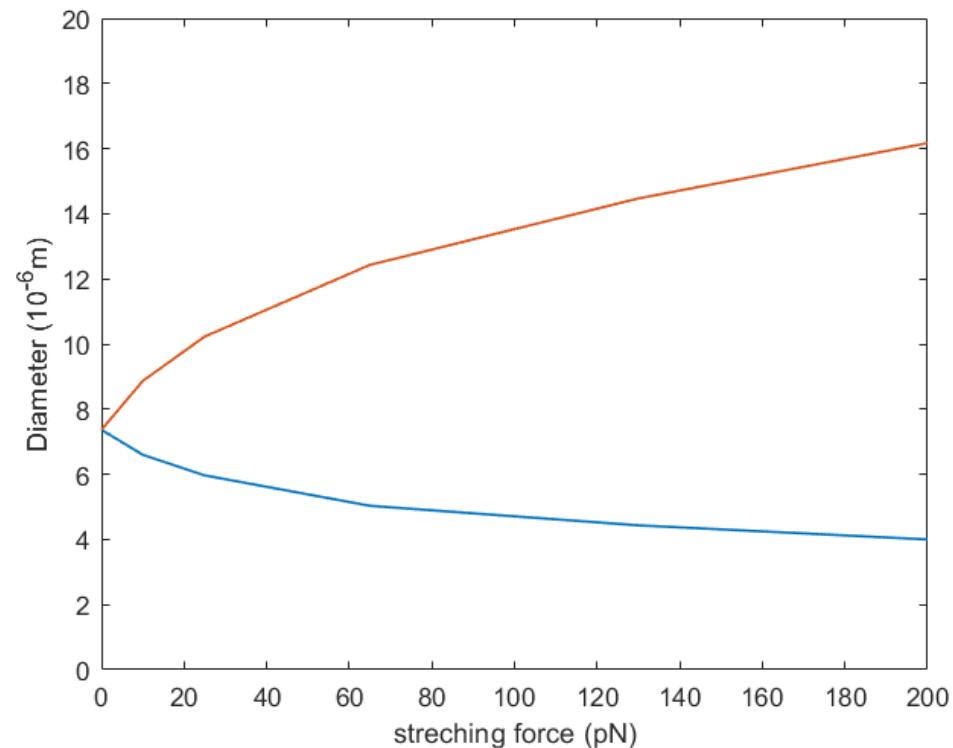


200pN

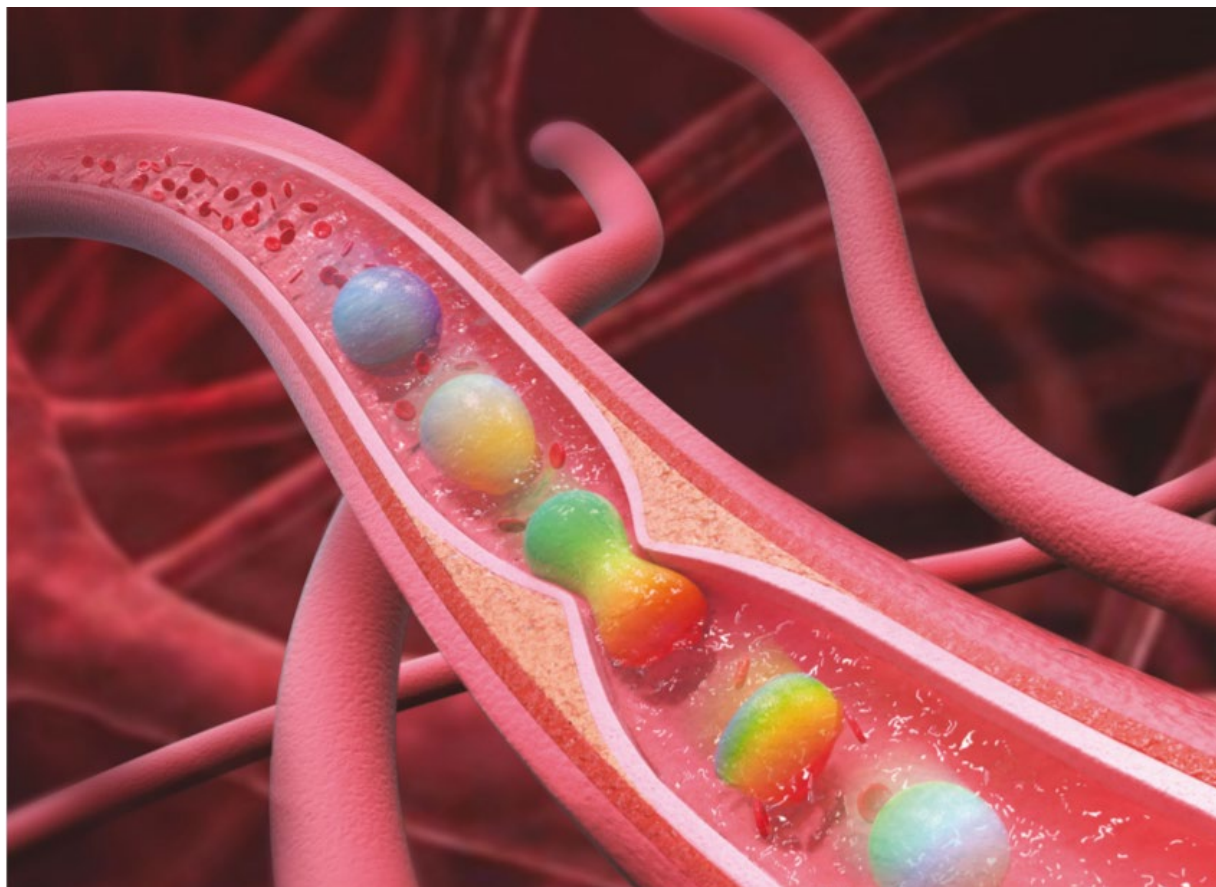
Nonlinear elastic and viscoelastic deformation with optical tweezers



[1]



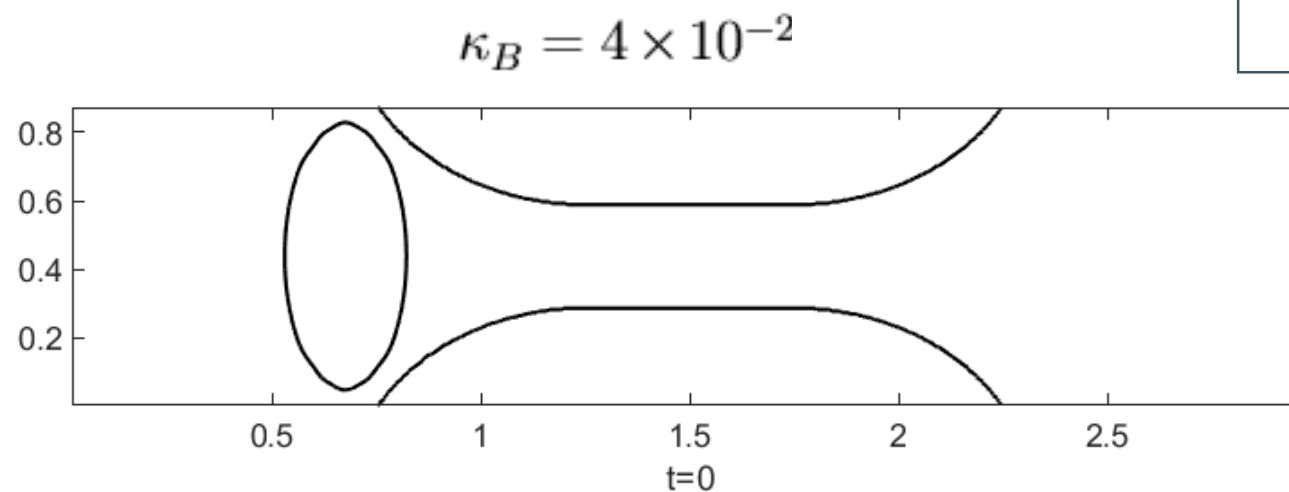
Vesicles through a Narrow Channel



Soft Matter, 2019, 15, 3307

Narrow gate passing: act of bending modulus

channel width=0.3
surface-area ratio: 11.4:1



$\kappa_B = 4 \times 10^{-1}$

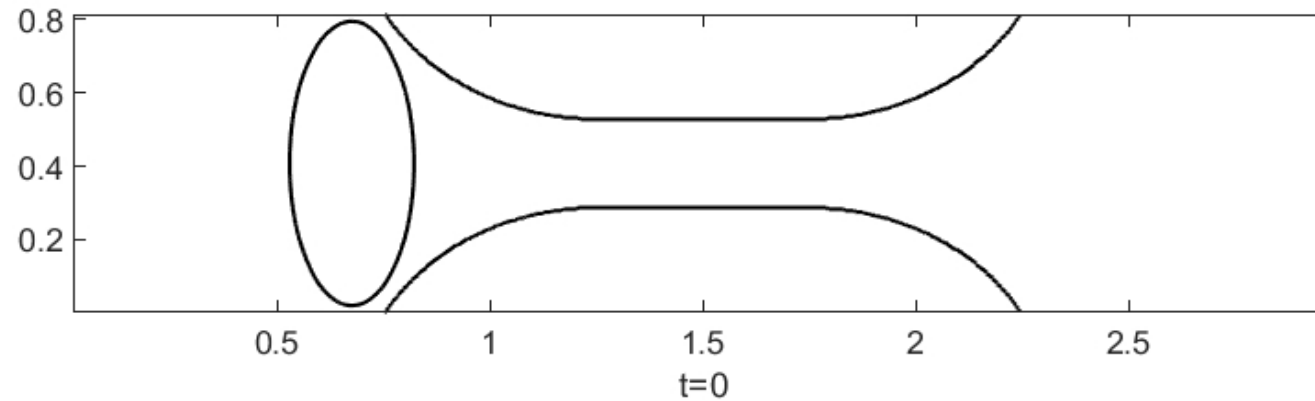


π

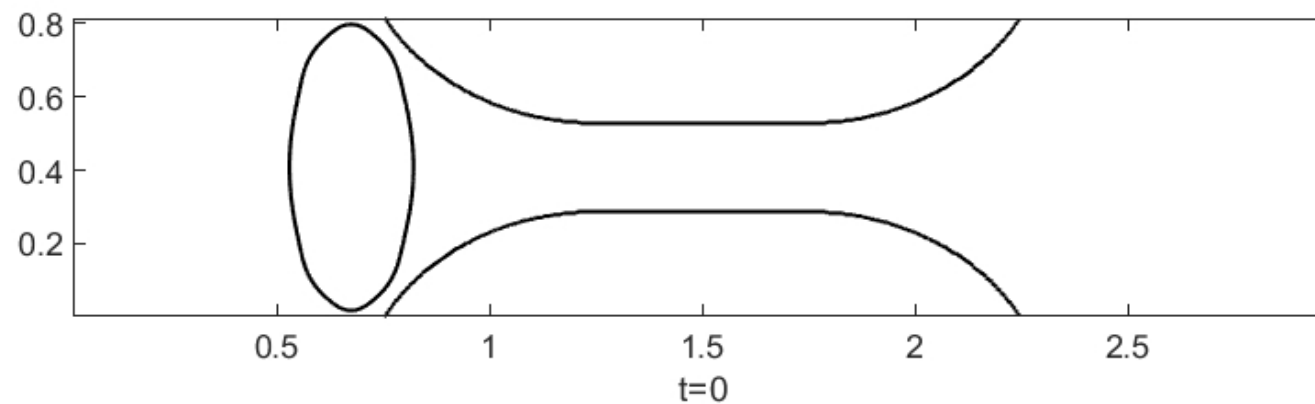
Narrow gate passing: act of channel width

channel width=0.24
surface-area ratio:
11.4:1

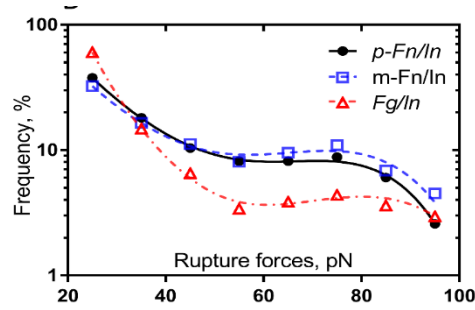
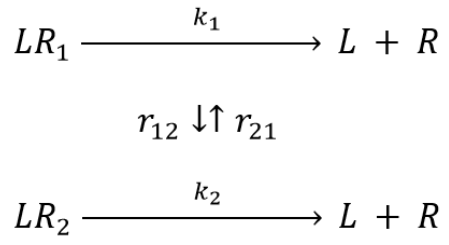
$$\kappa_B = 4 \times 10^{-2}$$



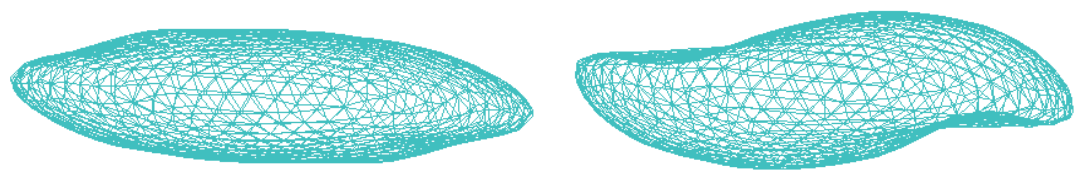
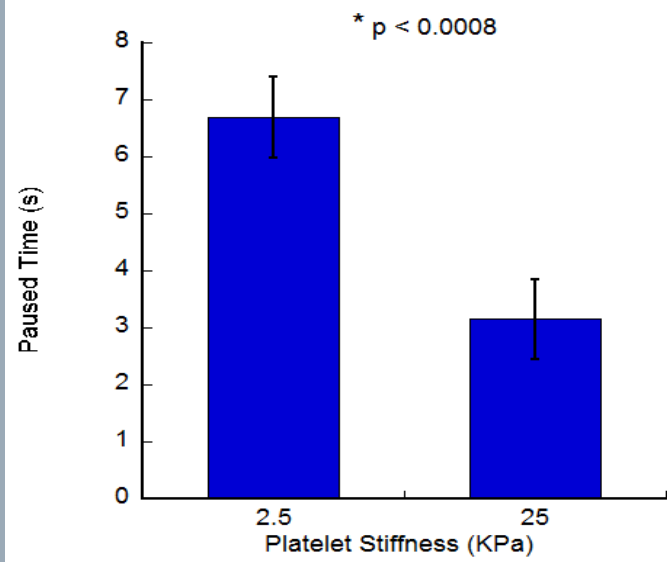
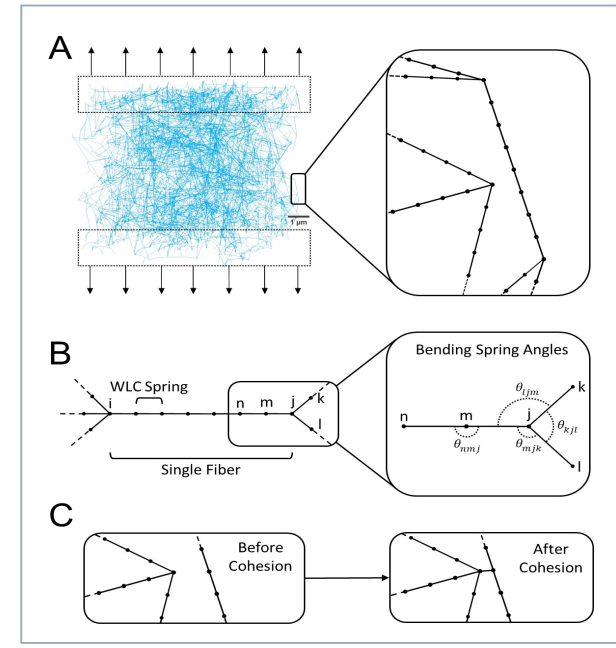
$$\kappa_B = 4 \times 10^{-1}$$



Other Models



(Left) The two-state kinetic model suggests allb β 3 exists in two interconvertible states, a lower affinity state R_1 and a higher affinity state R_2 . **(Right)** Experimental rupture force profiles (symbols) of the interactions of allb β 3 with polymeric fibrin (p-Fn), monomeric fibrin (m-Fn), and fibrinogen (Fg) fitted to the model.



The simulated deformations of platelet structures during their adhesion to the vessel wall for platelet stiffness of 2.5 KPa (a) and 25 KPa (b). The effect of the platelet membrane stiffness on the platelet paused time (c). The paused time was 6.69 ± 0.71 s (M \pm SD) for the membrane stiffness of 25 KPa, which was about twice higher than the paused time of 3.15 ± 0.69 s (M \pm SD) for the membrane stiffness of 2.5 KPa.

Concluding Remarks

We developed macro- and micro-scale models for studying various aspects of blood clotting processes.

1. A thermal dynamically consistent continuum model of mechanical stability of blood clot is introduced;
2. A thermal dynamically consistent model for deformable cells is derived;
3. An efficient energy stable 2nd order scheme is designed to solve the obtained cell system.